Universität Hamburg
DER FORSCHUNG | DER LEHRE | DER BILDUNG

Nanoparticles and Nanoclusters: Novel Performance in Life Science

Dissertation

zur Erlangung des Doktorgrades

an der Fakultät für Mathematik, Informatik und Naturwissenschaften

Fachbereich Physik

der Universität Hamburg

vorgelegt von

Lin Zhu

aus

Jiangsu, China

Hamburg

2019

Gutachter

Gutachter der Dissertation:	Prof. Dr. Wolfgang Parak
	Prof. Dr. Michael A. Rübhausen
Gutachter der Disputation:	Prof. Dr. Daniela Pfannkuche
	Prof. Dr. Wolfgang Parak
	Prof. Dr. Michael A. Rübhausen
	Prof. Dr. Robert Blick
	Prof. Dr. Nils Huse
Vorsitzender des Promotionsausschusses:	Prof. Dr. Michael Potthoff
Dekan der Fachbereichs Physik:	Prof. Dr. Heinrich Graener
Tag der mündlichen Prüfung:	06 August, 2019

Abstract

This cumulative dissertation focused on the investigation of nanoparticles (NPs) and nanoclusters (NCs), which are known for their extraordinary properties at the nanoscale. These nanomaterials have great potential for biological applications. More efforts were put into this subject during my PhD study, and these works are mainly divided into two parts: the enzymatic degradation on polymer shell of NPs as well as the fluorescence origin of Au NCs and Ag NCs.

Firstly, iron oxide NPs with core sizes around 4 nm were synthesized. Then, surface modification was performed by polymer coating and conjugation with different fluorophores using different chemistries. After exposing the modified NPs to several species of enzymes/enzyme mixtures, the degradation of the polymer shell can be observed through the dissociation of fluorophores from NPs. The results indicate the enzymatic cleavage percentage of the fluorophore-modified organic surface coating depends on the conjugation chemistry used and the types of enzymes to which the NPs are exposed. This work represents significant importance in forecasting the digestion of NPs in biological environment, and has relevance for NP-based in vitro and in vivo delivery or other potential applications.

In the second part, the photoluminescence properties of Au NCs and Ag NCs were intensively studied. By monitoring the in-site synthesis, the formation processes of these NCs were known. In addition, influences of capping ligands, metal core, oxidation state as well as solvent on their fluorescence were also largely investigated. By changing different physico-chemical parameters, their luminescence properties were also altered due to different mechanisms as described in this thesis. In these studies, a comprehensive understanding about the fluorescence origin of Au and Ag NCs is achieved. These fundamental knowledges enable us to tailor the NCs' luminescence, thus their applications in in vivo imaging can be advanced.

Zusammenfassung

Diese kumulative Dissertation konzentrierte sich auf Nanopartikel (NPs) und Nanocluster (NCs), die für ihre außergewöhnlichen Eigenschaften auf der Nanoskala bekannt sind. Diese Nanomaterialien besitzen ein großes Potenzial für biologische Anwendungen. Im Rahmen meiner Doktorarbeit wurden weitere Anstrengungen in diese Richtung unternommen, und diese Arbeiten gliedern sich hauptsächlich in zwei Teile: Den Abbau von Enzymen auf der Polymerhülle von NPs sowie den Fluoreszenzursprung von Gold (Au) und Silber (Ag) NCs.

Zunächst wurden Eisenoxid-NPs mit einer Kerngröße von etwa 4 nm hergestellt. Dann wurde eine Oberflächenmodifikation durch Polymerbeschichtung und Konjugation mit verschiedenen Fluorophoren unter Verwendung verschiedener Synthesemethoden durchgeführt. Nach der Exposition mit verschiedenen Arten von Enzymen/Enzymmischungen kann der Abbau der Polymerhülle durch Dissoziation von Fluorophoren aus NP beobachtet werden. Die Ergebnisse zeigen, dass der prozentuale Anteil der enzymatischen Spaltung der mit Fluorophoren modifizierten organischen Oberflächenbeschichtung von der Konjugationschemie und der Art der Enzymen abhängt, denen die NP ausgesetzt sind. Diese Arbeit hat Bedeutung für die Vorhersage der Verdauung von NPs in biologischer Umgebung und ist für die NP-basierte In-vitro- und In-vivo-Verabreichung oder andere potenzielle Anwendungen relevant.

Im zweiten Teil wurden die Photolumineszenzeigenschaften von Au-NCs und Ag-NCs intensiv untersucht. Aus der Beobachtung der In-Site-Synthese war der Bildungsprozess dieser NCs bekannt. Darüber hinaus wurden Einflüsse der Verkappungsliganden, des Metallkerns, des Oxidationszustandes sowie des Lösungsmittels auf deren Fluoreszenz weitreichend untersucht. Durch die Variation verschiedener physikalisch-chemischer Parameter wurden ihre Lumineszenzeigenschaften zusätzlich durch unterschiedliche Mechanismen variiert, wie in dieser Arbeit beschrieben. In dieser Arbeit wird ein umfassendes Verständnis des Fluoreszenzursprungs von Au- und Ag-NCs erreicht. Mit diesen grundlegenden Kenntnissen zur Kontrolle der Lumineszenz von NCs kann deren Anwendung auf die In-vivo-Bildgebung vorangetrieben werden.

List of publications

[1] **L Zhu**, B Pelaz, Indranath C, W.J. Parak. Investigating Possible Enzymatic Degradation on Polymer Shells around Inorganic Nanoparticles. Int. J. Mol. Sci. 2019, 20(4), 935.

[2] **L Zhu**, M Gharib, C Becker, Z Yeng, A.R Ziefuß, L Chen, A.M Alkilany et al. Synthesis of Fluorescent Silver Nanoclusters: Introducing Bottom-up and Top-down Approaches in a Single Didactic Laboratory Class. *J. Chem. Educ.* (under review)

[3] **L Zhu**, Indranath C, W.J. Parak. Effect of different physico-chemical parameters in photoluminescence of gold nanocluster. (in preparation)

[4] A.M. Alkilany, **L Zhu**, Horst Weller, A Mews, W.J. Parak, M Barz, N Feliu. Ligand density on Nanoparticles: A Parameter with Critical Impact on Nanomedicine. Adv Drug Deliver Rev (revision submitted).

[5] Huhn J, Carrillo-Carrion C, Soliman MG, Pfeiffer C, Valdeperez D, Masood A, **Zhu L** et al. Selected Standard Protocols for the Synthesis, Phase Transfer, and Characterization of Inorganic Colloidal Nanoparticles. *Chem Mat* 2017; 29:399-461.

Contents

1. Introduction

Nanoscience is now commonly known as a very promising and progressive field after explosive development. It has combined with physics, chemistry, electronics, optics and biology and raised a huge number of important issues, ranging from fundamental theoretical questions to technological applications. Generally speaking, nanoscience or nanotechnology is to control the synthesis of nano-objects with at least one dimension size between 1-100 nm (intermediate between single atoms or molecular structures and bulk materials [1]. In my thesis, the nano-objects are mainly referring to NPs and NCs (referring to ultrasmall NPs, ranging from subnanometer to ca 2nm). They obtain unique physical and chemical properties, which are different from those of their constituent parts (either atoms or molecules) and macroscopic pieces of matter.

Thanks to a great progress in nanotechnology in last decades, researchers have achieved great control of the size, shape and composition of various NPs and NCs. And by using various analysing tools such as TEM, AFM, NMR, IR spectroscopy in studying the characters of NPs and NCs, their structures and molecular compounds are able to be known [2]. However, there are still a number of unknown performances of these nanomaterials. Therefore, one research field is to research the mechanisms of nanomaterials´ novel properties. Only if we have a deep understanding of the origin of these properties can we take advantages of them and avoid their drawbacks at the same time.

Another hot research topic is to develop their applications in biology. To our knowledge of biology substances, cells (10-100 μM), viruses (20-450 nm), proteins (5-50 nm) and genes (2 nm wide and 10-100 nm long) have larger or comparable size to NPs [3]. In Figure 1, the size comparison of nanomaterials and some biological components are listed. The nanomaterials (e.g. liposome, fullerene, Dendrimer, carbon nanotube, graphene) are between the size of glucose molecule and virus. Because of analogous size between nanomaterials and these biological items, they can act as intrinsic drug agents and selectively perturb and modify cellular processes [4].

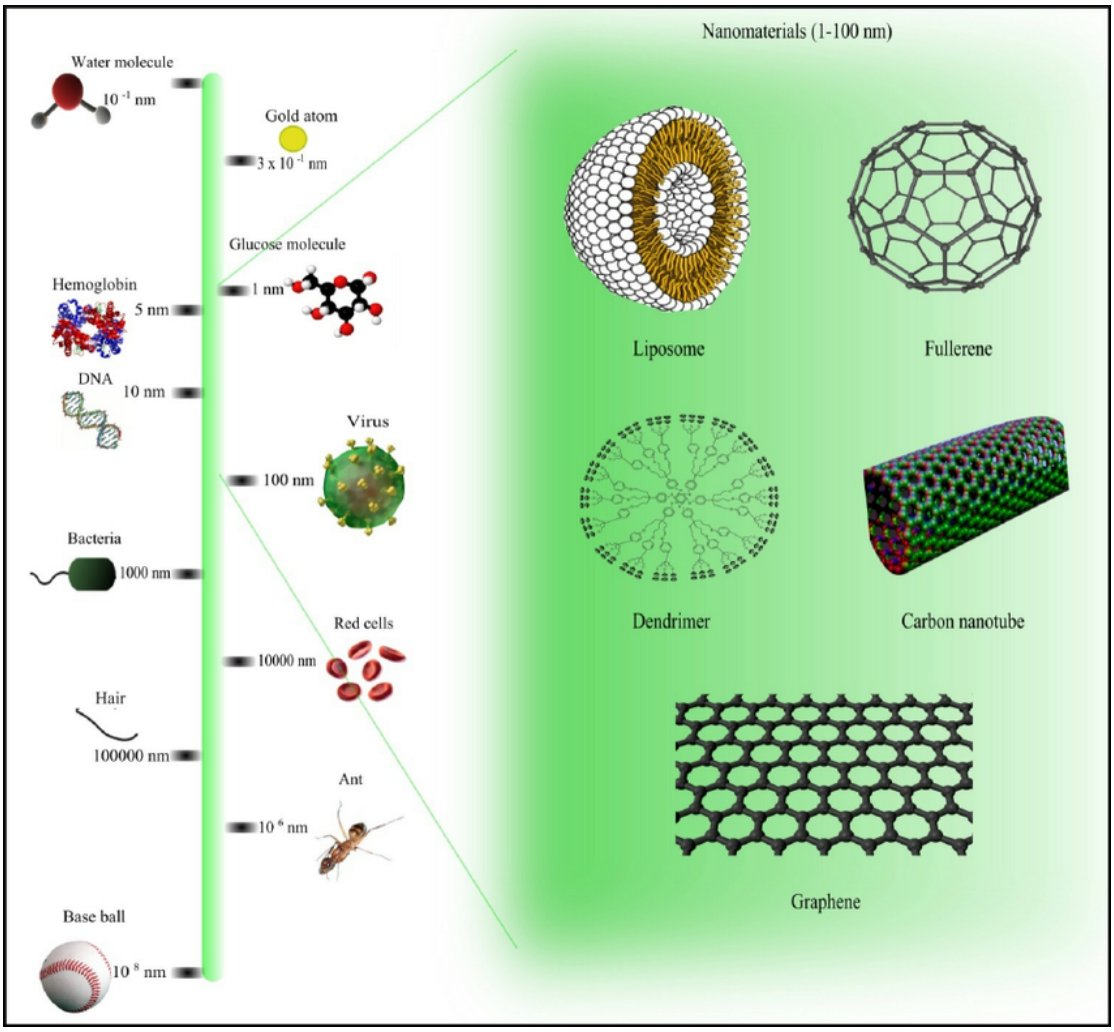

Figure 1. *Comparison of the sizes of nanomaterials with those of biological components and other common materials [5]. The right side displayed a variety of typical nanomaterials, the left side showed the ruler range from 10^{-1} nm to 10^{8} nm, which is the size from water molecule to base ball.*

As a hot spot in nanotechnology field, our research also focused on their performance for life science. This thesis contained two different research topics: one is to analyse the interaction between nanomaterials and basic components of biological systems (such as enzymes), another is to accumulate methods of controlling their particular characteristics for biological applications.

1.1 NPs

Since the term “NP” firstly appeared 30 years ago, a wide range of scientific reports in regards of the synthesis of nanostructured materials and their applications have been appearing. Nowadays, NPs, which are of great potential in various fields, has drawn much attention from scientists all over the world and developed by industries to be used in various fields in our daily life.

There are two approaches to the synthesis of NPs: “top-down” and “bottom-up” [6, 7]. “top-down” approaches refer to physical methods by breaking the bulk piece of metal into nanomaterials, and “bottom-up” approaches are usually by synthesizing the NPs from atomic or molecular species through chemical reaction, and then metal atoms were decomposed and generated to bigger size. The “bottom-up” approaches (including wet chemical synthesis, hydrothermal methods, reverse micelles, physical and chemical vapour deposition, etc.) are broadly used nowadays for a better control of size and shape. In 1950, LaMer and Dinegar explained the mechanism of synthesis process with atomic nucleation and size growth [8]. Firstly, the metallic precursor is generated to metal atom by reduction, but there are no nuclei produced in this process even metal atoms are saturated in solution. After the concentration of metal atoms become higher than a critical value, they start the self-nucleation. At this stage, some crystals gather together and form a number of nuclei, which are used as seeds to attract more atoms grow on them. When the NPs grow big enough, the smaller ones will also dissolve and assemble bigger NPs. Finally, the NPs will become uniform to have most stable state [9].

NPs can be classified into various groups according to their size, shape, composition or other properties. According to their composition, NPs can be prepared from metals (e.g. Au NPs, Ag NPs) [10], semiconductors (e.g. CdSe NPs, CdS NPs) [11], carbon (e.g. graphene, fullerenes) [12], polymers (e.g. Poly(lactic-co-glycolic acid) NPs, Polyethylene glycol NPs) [13], biologically derived substances (e.g. liposomes, bacteriophages) [14]. Au and Ag NPs are plasmonic NPs with fascinating optical properties in a wide spectral range from visible to NIR range, which has been actively studied for photothermal therapy [15]. Semiconductor NPs, also named as quantum dots, are luminescent with application in optical sensing, bioassays, and as photoluminescent imaging contrast agents [16]. Magnetic

NPs such as Fe_3O_4 and FePt have attracted great interests in the field of magnetic resonance imaging, data storage, and environmental remediation [17]. They show superparamagnetic behaviour when the size of the NPs is below a critical value (typically around 10-20 nm) [18]. In nature, there are also self-assembled biological molecules, e.g., peptides can be further organized to form nanowires, nanotubes and NPs via their molecular recognition function [19]. Through this recognition function, these biological molecules can also be addressed the nanomaterials to exact locations [20].

NPs with various shapes such as spherical, rods, cube, triangular, hexagonal were also designed. The incredible properties of NPs also strongly depend on shape of NPs. Most of these studied NPs are spherical, which contain the minimum surface at the same volume to keep thermodynamically stable [21]. According to report, shapes of NPs also depend on their interaction with stabilizers and the inductor around them as well as the preparation method. Platinum NPs with cubic shape are formed by the help of sodium polyacrylate for control of the shape. It can also stop the growth of the particles at small size distribution and prevent the NPs from coalescing with each other, causing better monodispersity. Sun reported the method the reduction of silver nitrate with ethylene glycol at the presence of a capping reagent poly(vinyl pyrrolidone), which can finally yield bicrystalline Ag nanowires [22]. With ultraviolet irradiation photoreduction process, morphology of Au NPs are interfered by the concentration of Au cations, the irradiation time and also the species of polymer capping materials [23].

With the evolving synthesis methods, NPs can be synthesized in water, chloroform, toluene or other organic solvents. Mostly, for the application in biology, the NPs need to be dispersed in water and sustain colloidal stability after the synthesis. Nevertheless, the syntheses in organic solvent are usually can be made in higher concentration with improved monodispersity [9]. Thus, various NPs are firstly produced in organic solvents and then transferred to aqueous solutions. A range of methods for phase transfer were reported. One of the phase transfer method is using capping molecules to modify the surface of the NPs to obtain hydrophilicity [24]. For example, Au NPs protected by weakly bound ligand such as dodecylamine protected can perform ligand exchange with strong ligands like mercaptopropionic acid or mercaptoundecanoic acid to perform phase transfer [25]. Polymer coating is another good method of phase transfer by wrapping the NPs with

amphiphilic polymers. The hydrophobic parts of the polymer have good affinity to the surface of the NPs, and the hydrophilic parts can provide good colloidal stability of NPs in aqueous solution. For example, a variety of NPs are coated with poly(D,L-lactide), poly(lactic acid), poly(D,L-glycolide), poly(lactide-co-glycolide), poly(cyanoacrylate) and so on [25].

1.2 NCs

NCs are very important compositions in nanoscience, which are aggregates of several or tens of atoms, typically around 2 nm, behaving like molecules [26, 27]. NCs are of great value in nanotechnology research with the potential usage in catalysis, sensing, imaging, optics, energy conversion and also biomedicine [28]. NCs are aggregates of several or tens of atoms, typically around 2 nm, behaving like molecules [26, 27].

In terms of their synthesis methods, NCs can be classified to several groups such as molecular, gas-phase, colloid, solid-state, matrix and film clusters [29]. For example, molecular clusters can be prepared by chemical reactions; gas-phase clusters can be synthesized by laser vaporization; synthesis of colloid clusters are usually formed in solution upon chemical reaction; solid-state NCs can be prepared by photochemical reactions or mechanochemical transformations; matrix clusters are prepared by using matrix methods; nanofilms are prepared broadly by using laser vaporization and molecular beams such as CVD [29]. Meanwhile, different categories of NCs maybe compound together by different kinds of forces: attractions between oppositely charged ions (e.g. NaCl clusters), van der Waals attractions (e.g. He and Ar clusters), covalent chemical bonds (e.g., Si clusters), or a metallic bonds (e.g. Au and Ag Clusters) [30].

As it known to all, there are no two NPs exactly the same and it is an obstacle for us to understand precisely the fundamental properties of NPs [28]. To solve this problem, a certain types of NCs, including molecular metal clusters, van der Waals noble gas and water clusters, gas-phase metal clusters and fullerenes, were designed with specific number of atoms with specific structures [29]. These clusters are based on cores with specific “magic” numbers of metal atoms bound directly to one another and surrounded by ligands. Due to

the "magic" numbers, the clusters can be formed in more stable structures in accordance with the close-packing pattern similarly to bulk metal [31]. When the clusters need to form a 12-vertex polyhedron (cuboctahedron, icosahedron or anticubooctahedron), the "magic" numbers (N) can be found from the formula:

$$\mathrm{N} = \frac{1}{3}(10n^3 + 15n^2 + 11n + 3)$$

Where n is the number of layers around the central atom. Therefore, this gives a set of "magic" numbers N=13, 55, 147, 309, 561, 923, 1415, etc. [31]

In our research, we focus on the water-soluble metal NCs, which are reported to have electrochemiluminescence [32]. They were firstly defined by Cotton in 1960s, and metal NCs such as Au, Ag, Cu, Pt, Pd were synthesized and studied since then [33]. For their synthesis, the reduction of metal ions are one of the most commonly used synthesis methods, such as reducing Au^{3+} with $NaBH_4$. However, small NCs have the tendency to aggregate and form large NPs. To different synthesis, suitable capping agents are needed to protect the NCs.

1.3 Biological applications

One of the most prominent application of nanotechnology is biomedicine. The research of biomedical application of NPs and NCs have been carried out for decades [34, 35]. The possible applications of nanomaterials are listed as: fluorescence biological labels, drug and gene delivery, bio detection of pathogens, detection of proteins, probing of DNA structure, tissue engineering, tumour destruction via heating (hyperthermia), separation and purification of biological molecules and cells, MRI contrast enhancement, phagokinetic studies, etc. [36].

For example, PLGA NPs as one of the most extensively investigated biodegradable NPs have been evaluated for sustained and targeted/localized delivery of different agents including plasmid DNA, proteins, peptides and low molecular weight compounds [37]. Au NPs with high efficient conversion of light into heat can allow for the highly specific thermal ablation of diseased or infected tissues [38]. Compared with organic fluorophores,

quantum dots that feature large molar extinction coefficient, high quantum yield, narrow emission bandwidth, size-dependent tunable emission and high photostability are attractive as alternative luminescent labels for optical labelling and imaging [39].

For NCs, they were explored for the application in biodetection (such as the detection of metal ions, small biomolecules, proteins, nucleic acids) [40]. And metal NCs have great advantages in application for biological imaging, because of their stability, good biocompatibility and brightness [41]. In addition, large Stokes shift of Metal NCs can prevent spectral cross-talk to have sensitive detection signal [41]. Among these reports, Wang invented a new aqueous-phase approach to prepare Ag_2S NCs with the property of turning the photoluminescence from the visible red to near infrared period [42]. The NCs were synthesized using glutathione as a scaffold showed low cytotoxicity and in the following FT-IR spectroscopy measurement. The Ag_2S NCs showed the potential to be used as a probe for real-time optical cellular imaging.

Furthermore, a quantity of products using nanotechnology has been appearing in consuming market. According to the Nanotechnology Consumer Product Inventory, 1814 products from 622 companies in 32 countries were listed in 2015, in which the health and fitness category contains the most part [43]. In addition, another inventory (The Nanodatabase) listed 1423 products that are available in the European consumer market [44]. Apart from a high fraction of products with unknown nanomaterial composition, silver nanomaterials are the most frequently advertised nanomaterial components due to their antimicrobial properties. From Table 1, a number of nanomaterials from same research institution and companies for bio- and medical application were listed. Most of these products are for drug delivery, tagging biomolecules, labelling cellular parts, tissue engineering and orthopaedics [36]. In total, there are more and more advancing applications of nanotechnology in medicine, thanks to constant devotion from researchers in scientific institutions and medical companies.

***Table 1**: Commercial product list of nanomaterials for bio- and medical application [36].*

Company	Major area of activity	Technology
Advectus Life Sciences Inc.	Drug delivery	Polymeric nanoparticles engineered to carry anti-tumour drug across the blood-brain barrier
Alnis Biosciences, Inc.	Bio-pharmaceutical	Biodegradable polymeric nanoparticles for drug delivery
Argonide	Membrane filtration	Nanoporous ceramic materials for endotoxin filtration, orthopaedic and dental implants, DNA and protein separation
BASF	Toothpaste	Hydroxyapatite nanoparticles seems to improve dental surface
Biophan Technologies, Inc.	MRI shielding	Nanomagnetic/carbon composite materials to shield medical devices from RF fields
Capsulution NanoScience AG	Pharmaceutical coatings to improve solubility of drugs	Layer-by-layer poly-electrolyte coatings, 8–50 nm
Dynal Biotech		Magnetic beads
Eiffel Technologies	Drug delivery	Reducing size of the drug particles to 50–100 nm
EnviroSystems, Inc.	Surface desinfectsant	Nanoemulsions
Evident Technologies	Luminescent biomarkers	Semiconductor quantum dots with amine or carboxyl groups on the surface, emission from 350 to 2500 nm
Immunicon	Tarcking and separation of different cell types	magnetic core surrounded by a polymeric layer coated with antibodies for capturing cells
KES Science and Technology, Inc.	AiroCide filters	Nano-TiO2 to destroy airborne pathogens
NanoBio Cortporation	Pharmaceutical	Antimicrobal nano-emulsions
NanoCarrier Co., Ltd	Drug delivery	Micellar nanoparticles for encapsulation of drugs, proteins, DNA
NanoPharm AG	Drug delivery	Polybutilcyanoacrylate nanoparticles are coated with drugs and then with surfactant, can go across the blood-brain barrier
Nanoplex Technologies, Inc	Nanobarcodes for bioanalysis	
Nanoprobes, Inc.	Gold nanoparticles for biological markers	Gold nanoparticles bio-conjugates for TEM and/or fluorescent microscopy
Nanoshpere, Inc.	Gold biomarkers	DNA barcode attached to each nanoprobe for identification purposes, PCR is used to amplify the signal; also catalytic silver deposition to amplify the signal using surface plasmon resonance
NanoMed Pharmaceutical, Inc.	Drug delivery	Nanoparticles for drug delivery
Oxonica Ltd	Sunscreens	Doped transparent nanoparticles to effectively absorb harmful UV and convert it into heat
PSiVida Ltd	Tissue engineering, implants, drugs and gene delivery, bio-filtration	Exploiting material properties of nanostructured porous silicone
Smith & Nephew	Acticoat bandages	Nanocrystal silver is highly toxic to pathogenes
QuantumDot Corporation	Luminescent biomarkers	Bioconjugated semiconductor quantum dots

1.4 Challenge and research goal

As the goal for medical application, one focus of nanomaterials was the biological in vitro or in vivo evaluation. Innovation of NPs are urgently needed to derive the benefits from their outstanding properties while limiting the adverse health impacts [45]. After going inside human body (by inhalation, oral administration, dermal exposure and injection), NPs or NCs will reach different organs, contacting tissues and cells as illustrated in figure 2, and their hazard assessments should be carried out at systemic level, tissue/cell level and molecular level [46, 47]. Considering the small size and large surface area of NPs or NCs, they have much higher surface reactivity and greater biological activity than bulk materials. NPs can trigger cytotoxic effects either by releasing toxic ions or by generating ROS [45, 48, 49]. And after exposure in lungs or other organ systems after inhalation, the

NPs or NCs have unexpected interactions with the body. Comparing with bulk materials, they may change their body distribution, passage of blood brain barrier, and trigger blood coagulation pathways [50]. For their future application in life science, plenty of such risk assessments should be made to avoid the potential hazards. Assays such as toxicology, materials science, medicine, molecular biology, and bioinformatics are essential [51]. In a word, for the use of nanotechnology in medicine, deep and all-round tests are urgently needed to reduce the toxicity and side effects of nano-objects.

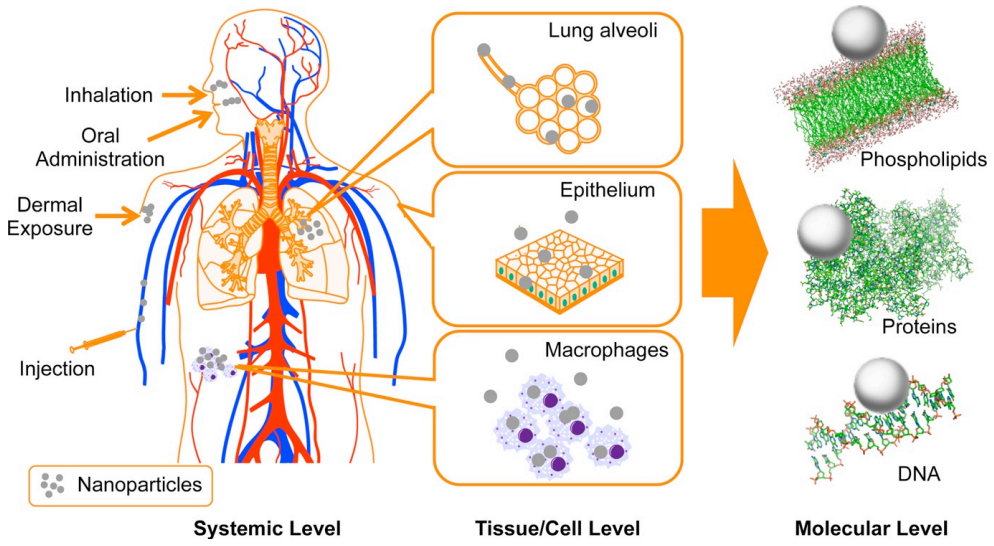

Figure 2. *Interactions of NPs with biological systems at various levels. After entering the human body through different passways, the association of NPs with biological items at systemic level, tissue/cell level and molecular level should be thoroughly understand [47].*

Another high spot in nanoscience is synthesizing novel NPs or NCs to obtain unique characteristics. For example, with the capability of tailoring silica NPs with mesoporous structure, they have high loading capacity for drug and gene [52]. And these NPs can also designed to comprise moieties responsive to redox, pH or enzyme cleavable in order to allow a safe excretion from the body [53]. In another way, adjustments of composition, shape, size, or other parameters of nanomaterials also deserve to have a deep understanding of their performance and filtrate them for proper use. For instance, Prashant reported the absorption and scattering properties of different NP species (Au nanospheres, silica-gold nanoshells and gold rods at different size), and their studies approved that Au nanorods can

be the best choices as agents for bioimaging and photothermal therapy due to their most superior NIR absorption [54]. Finally yet importantly, to understand internal mechanisms of nanomaterials by different synthesis methods are of great value. A large number of reports on emerging new species of NPs and NCs are lack of related theory, and many novel phenomena are still need to be fully explained.

In conclusion, it has already gained some achievements for the applications of nanotechnology as we discussed above. However, the real commercial application of nanomaterials are still very limited and various excellent properties of these nanomaterials still deserve continuous devotions in nanomaterial tailoring and biological safety guarantee. The studies written in this thesis are also on the goal to improve the understanding of NPs and NCs in these aspects for their future application.

2. Analysis and characterization methodology

2.1 UV-Vis spectroscopy

UV-Vis spectroscopy is a technique to quantify the light absorption by a sample, which is also known as absorption spectroscopy or reflectance spectroscopy. The UV-Vis spectroscopy (Agilent 8453) in our lab can collect the spectra from 200 nm to 1100 nm across the ultraviolet, visible and near IR region. The simplest method to measure the absorption of a sample is to detect the intensity of a beam light before and after passing through the sample. The value of Absorption (A) is calculated by:

$$\mathrm{A} = -\log_{10}\frac{I}{I_0}$$

I is the light intensity of light after its passing through the sample, I_0 is the intensity of incident light. And before the sample measurement, a "blank" sample with only the dispersing medium is used to subtract the influence of the solvent. Then, the measurements at each wavelength will be analysed, and the final absorption spectrum will be exhibited with absorption versus wavelength.

UV-Vis spectroscopy is one of the elementary equipment for the quantitative analysis of transition metal ions, conjugated organic compounds, biological macromolecules and so on. It is also a very significant tool to identify and characterize for NPs, especially for Au and Ag NPs, since they have unique absorption spectrum due to their surface plasmon resonance property [55, 56]. These plasmonic NPs absorb radiations of visible to near infrared region depending on the size and shape of NPs, resulting in different peaks in the UV-Vis absorption spectrum [57]. Haiss W examined a series of spherical Au NPs with the size ranging from 5 nm to 100 nm [58]. The correlation between particle size and wavelength was highly consistent in both theory and experiment. Equations of position of the surface plasmon resonance peak and ratio of absorbance at surface plasmon resonance peak (A_{spr}) to the absorbance at 450 nm (A_{450}) were calculated in dependence of the NP diameter. Besides, with the help with UV-Vis absorption spectrum, concentration of NPs can be determined according to Beer-lambert law [59]. The concentration of sample (C_{NP}) is calculated by the equation:

$$C_{NP} = \frac{A}{\varepsilon \times l}$$

Here A is the absorbance of NPs, ε is the molecular extinction coefficient of NPs, and l is the path length of the cuvette, which is 1 cm in our experiments. There are already multiple reports presenting tables of extinction coefficient data for different NPs in different size [59, 60].

UV-Vis spectroscopy has also been reported extensively to study the tuning of optical properties and kinetics of NP synthesis [61, 62]. For example, Kim et al. synthesized Au NPs in the presence of preformed spherical hydrogel particles [63]. With the growth of NPs, their surface plasmon band is red shifted. With the help of the UV-Vis spectroscopy, precise size control of the encapsulated gold core can be realized. In another work, the swelling and deswelling behaviour of the pH sensitive polymer brushes with immobilized gold nanorods was observed by UV-Vis spectroscopy with a significant displacement of 32 nm in the longitudinal plasmon band [64].

It is also available to check the aggregation state of the NP sample in UV-Vis absorption spectrum. The conduction electrons near each NP surface become delocalized and shared with neighbour NPs when the NPs aggregate, resulting in the surface plasmon resonance shifting to lower energies [65]. In the UV-Vis absorption spectrum, the red shift of the absorption and the broader absorption peak are usually witnessed. Meanwhile, the baseline may also elevate due to scattering by aggregates. In total, the UV-Vis spectroscopy is a very essential and intensively used device in the characterization of NPs.

2.2 DLS

DLS is widely used in nanomaterial analysis to determine the hydrodynamic diameter of NPs or NCs, referring to the particle size in solution. DLS system contains the following components: a laser providing the light source to illuminate the sample, an attenuator to reduce the intensity of the laser source, the detector to measure the light scattered by the sample, a correlator undergoing digital process and finally a computer with software to analyse the data. DLS requires information about diffusion coefficient of samples and

viscosity of the solvent. One of the advantages of DLS to gain the size of nano-objects comparing with TEM is its invasiveness. The sample is prepared in solution with little manipulation and can be recovered after analysis [66]. Other advantages are the demand of low volume of samples and the possibility to measure particles size across the range from 0.1 nm to 10 μm.

In the measurements, the velocity of Brownian motion, which is defined by a property known as the translational diffusion coefficient (D), is related to the size (d(H), hydrodynamic diameter) using Stokes-Einstein equation:

$$d(H) = \frac{kT}{3\pi\eta D}$$

In this equation, k is Boltzmann´s constant, T is absolute temperature, and η is viscosity. Based on this equation, larger NPs or NCs feature slower the Brownian motion.

In DLS analysis, the obtained distribution of diameter can be plotted versus the number and volume of nanomaterials, and the intensity of the scattered light. As larger particles can scatter much more than smaller ones, the intensity distribution can be overestimated in the amount of large NPs. Only a little amount of aggregation in Au NP will also scatter a lot and result in a peak in higher size. In our projects, we chose the hydrodynamic size with number distribution.

2.3 LDA

LDA, also known as laser doppler velocimetry, is the technique to measure zeta potential by using the well-known doppler shift in a laser beam to measure the velocity in fluids. The equipment has the advantages such as no-invasive, high spatial and temporal resolution. During the measurements, a voltage is applied across a pair of electrodes at two sides of the cuvette for storing samples. And the electrophoretic mobility of these nanomaterials are measured. Finally, the electrophoretic mobility is used as the sources of data to calculate zeta potential [67].

Zeta potential is the potential difference across phase boundaries between solids and liquids [68]. NPs have the surface charge, which can attract a layer of ions of the opposite

charge, and the electric potential at the boundary of the double layer is known as the zeta potential. DLS is mainly used to measure the repulsion and attraction between particles as well as the dispersion stability of colloidal systems [69]. If the NPs or NCs have a large zeta potential value (negative or positive), they will repeal each other and have good dispersion stability. And the dividing line between stable and unstable aqueous dispersion is either +30 mV or -30 mV [68]. Due to the Van der Waal inter-particle interaction, nanomaterials with low zeta potential will gradually aggregate.

2.4 Fluorometer

Fluorometer is a rapid and sensitive facility to measure fluorescent properties of samples including intensity and wavelength distribution after excitation by a certain spectrum of light ranging from UV (200~400 nm), visible (400~700 nm) to near IR (700~1100 nm). In a fluorometer, after the light source emits a wide range of light, a filter or monochromator will select out a defined group of excitation wavelengths. Then, the samples are excited and emit light at other wavelengths. Subsequently, the light that goes through the sample is collected and pass through another filter or monochromator to remove the emission wavelength. Finally, the emitted light is measured by a detector.

Luminescence emission of a sample after excitation by ultraviolet or visible light photons is depending on their excited state and emission pathway. After the absorption of light, the emitted light occurring within nanoseconds has a longer wavelength and lower energy. The fluorometer can be used not only for measuring parameter of fluorescence, but also for identify the presence or calculating the amount of specific fluorophore [70].

2.5 TEM

To further investigate the core size and morphology of the nanomaterials, TEM (Jeol JEM3010) was used in our experiments. In each measurement, 3 μL of each sample were dropped to a carbon-coated copper grid, and the samples were dried spontaneously at room

temperature. Finally, their images were recorded by TEM and a free software named ImageJ can be used to obtain an average diameter of the samples.

2.6 ICP-MS measurements

ICP-MS is used to detect the concentration of metals and some other non-metals. An Agilent ICP-MS 7500cs inductively coupled plasma-mass spectrometry instrument was used for this purpose. Firstly, samples are diluted to 500 µL, and 50 µL of the solution is taken from each part and digested with 150 µL of freshly prepared aqua-regia. The mixture is kept on a shaker for 2 h. The digested samples are further diluted by 2% of HCl and then used for the ICP-MS analysis. After measuring the elemental metal concentrations, the molecular concentration of spherical NPs then can be calculated. Firstly, the mass of a single NP core (m_{NP}) is calculated via the equation below:

$$m_{NP} = \rho * V_{NP} = \rho * 4/3 * \pi * (d_c/2)^2$$

ρ is the density of the materials, V_{NP} is the volume of one NP, d_c is the diameter of the NP core, which can be obtained after statistical analysis of TEM images.

Then, the mass of one mole of NPs (M_{NP}) can be calculated by multiplying the mass of a single NP core (m_{NP}) by the Avogadro number (N_A=6.022×10^{23} mol^{-1}). Finally, the molar NP concentration (c_{NP}) of the NP samples was obtained by dividing the mass concentration of the NPs as obtained by ICP-MP (C_{NP}) by the mass of one mole of NPs (M_{NP}).

3. Enzymatic degradation on polymer shell around inorganic NPs

3.1 Motivation

The first project I have done in my PhD is on the possible enzymatic degradation on polymer shell (published, doi: 10.3390/ijms20040935). The NPs with various functions such as imaging, labelling and drug release have been mostly studied. In order to realize these functions, there are various successfully used physical and chemical methods for linking DNA, biotins or dyes to NPs directly or to its external surface, which mainly include electrostatic adsorption, hydrophobic attraction, formation of covalent bonds, etc. However, except these studies, how these conjugations work in biological systems has not been intensively and thoroughly studied. This work is to research on enzymatic digestion of various bonds used in NPs.

After NPs entering organisms, they will be exposed to different local environments due to their trajectory. For example, acidic pH environment (in endosomes/lysosomes), may degrade NPs [71]. Enzymes may digest parts of the surface coating of the NPs, which can modify their physicochemical properties and consequently also their biodistribution [72, 73]. NPs in general are hybrid materials comprising different entities such as core materials, surface functionalization, and the corona of adsorbed biomolecules (in particular proteins) [74]. Specific enzymes may initiate enzymatic reactions of disparate parts of NPs [75]. Enzymatic degradation thus may be selective to specific parts of the NPs. For example, Sée et al. reported the separation of biological molecules from the surface of NPs through peptide bond cleavage by the protease cathepsin L in endosomal compartments [76]. Degradation of polymeric NPs consisting of poly(-glutamic acid) and l-phenylalanine ethylester by pronase E, protease, cathepsin B and lipase was also reported, resulting in an decreased NP size [77]. As it has been pointed out, degradation of the surface chemistry of NPs may have profound effects on their physicochemical properties, involving in particular loss of colloidal stability and change of the protein corona.

Moreover, enzymatic degradation of NPs can be also used for time-delayed delivery, where molecular cargo is only released after enzymatic degradation of a carrier matrix which encapsulated the cargo [78]. NPs can be formulated in this way to release cargos through enzymes which are only locally present at the target environment. For instance, a polymer/DNA complex for gene therapy was fabricated, in which 4-acetoxybenzyl ester groups are hydrolyzed by esterases, inducing charge-reversal and gene delivery [79]. A better understanding of enzymatic degradation of NP surface chemistries thus also may help for improved degradable delivery vehicles.

In our study, we focused on covalent bonds to attach different dye markers to NPs in parallel. We chose some very common bonds such as EDC and click reaction for trial. After synthesizing Fe_3O_4 NPs, we modified the surface with PMA and some specific ligands. By covalent bonds, different markers can be linked to these ligands. Finally, the stability of the NPs will be examined with a set of enzymes and biomolecules. In this study, we investigated enzyme-specific cleavage of distinct bonds present in the surface of NPs in more detail in order to probe possible enzymatic cleavage of these ligands from the NP surface [71]. This research can help us understand the performance of NPs that comprise some special bioconjugation strategies in the presence of enzymes, which is also valuable for enzyme-induced delivery.

3.2 Fe_3O_4 NPs and its application

In this project, Fe_3O_4 NPs are selected due to their good biocompatibility, superparamagnetic behaviour and chemical stability. Iron plays a significant role in biology, and it is a cofactor in the metabolism of hundreds of proteins and enzymes, involved in diverse body functions, such as oxygen transport, DNA replication, and cell cycle progression [80]. The human body contains 3-5 g of iron per person, and needs the intake of 20-25 mg every day (approximately 0.5 mg/kg). Due to the electrons spinning and orbital motion, materials made by Fe_3O_4 have ferrimagnetic behavior with opposing magnetic moments inside, the opposing moments are unequal and a spontaneous magnetization remains. When the temperature is below the Curie temperature, ferrimagnets hold a

spontaneous magnetization. For the super small ferrimagnetic NPs, they can obtain superparamagnetism, for which magnetic reversal can be thermally activated. Yang investigated the magnetic properties of Fe_3O_4 NPs from 2 to 14 nm with narrow size distribution. The NPs are ferrimagnetic at 10K, and become superparamagnetic at room temperature [81].

Iron oxide NPs with good biocompatibility and superparamagnetic behaviour can be a powerful non-invasive tool in biological applications. They can be linked with drugs, proteins, enzymes, antibodies or nucleotides and be delivered to the target organs, tissues or tumours by manipulating an external magnetic field [82]. The size and magnetic properties of iron oxide NPs also enable their applications as molecular imaging probes and as contrast enhancing probes for MRI [83]. By alternating an external magnetic field, iron oxide NPs can generate heat for hyperthermia [84]. Besides, other applications such as tissue repair and magnetofection were also reported [84, 85].

The introduction and functionalization of superparamagnetic iron oxide NPs are illustrated in Figure 3, in which Fe_3O_4 NP is one of the most important types. Mostly, these NPs are composed of inorganic iron oxide core and hydrophilic coating (e.g. dextran, carboxydextran, carboxymethyldextran, etc.). The figure also demonstrates the structure sketch of a hydrophobic core of superparamagnetic nanocrystallites, therapeutic hydrophilic shells and targeting ligands, which are utilized for imaging and therapy applications. For example, Saboktakin designed a kind of MRI detectable iron oxide NPs, which can carry several molecules such as drug and peptides [86]. It is possible to realize the multifuctionalization of the NPs for diagnosis and therapy, and this would be a great platform for the patients with cancer.

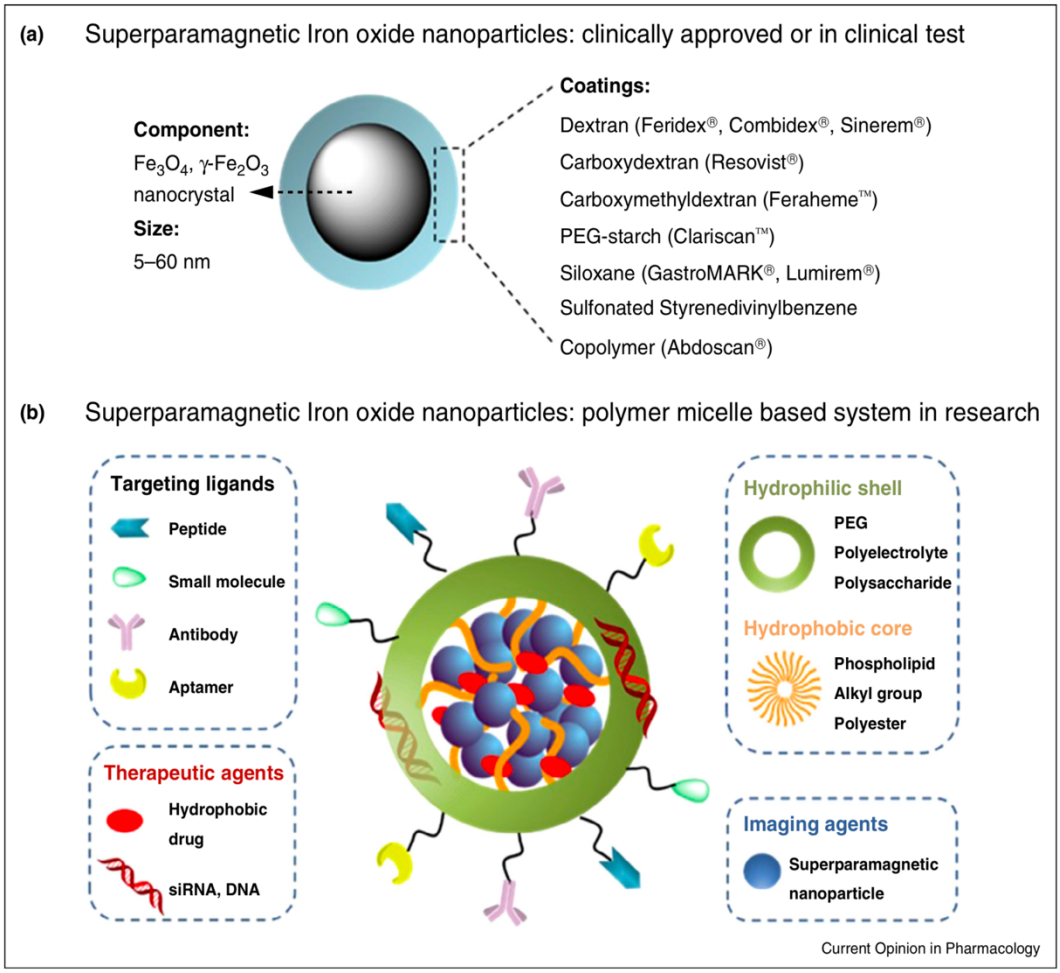

***Figure 3**. Schematic illustration of the composite system of surface-engineered iron oxide NPs for imaging and therapy applications [87].*

3.3 Synthesis and surface modification of Fe_3O_4 NPs

To synthesize Fe_3O_4 NPs with a diameter of ~4 nm, a thermal decomposition reaction was performed through a high temperature reaction of iron(III) acetylacetonate with 1,2-hexadecanediol in the presence of oleic acid, following the methodology reported by Sun *et al* [88]. After the synthesis, Fe_3O_4 NPs were surface modified as illustrated in Figure 4. Then, polymer coating was carried out in chloroform using three different polymers, and these coated NPs were subsequently conjugated with fluorophores. Different chemistries including EDC reaction and "click chemistry" (CuAAC reaction and Diels-Alder reaction) were carried out. In fact, click chemistry usually takes place at room atmosphere and is

insensitive to water and oxygen, and these chemistries have been used to synthesize multiple biomaterials. In this experiment, CuAAC reaction and Diels-Alder reaction were performed for the linkage of Fe_3O_4 PMA-Prop NPs with Coumarin and Fe_3O_4 PMA-Furf NPs with Cy5.5, respectively. In case of PMA-Prop-coated NPs, Coumarin 343-azide dye was linked by connecting the azide group of the dye with the alkyne group of Prop, forming 1,4-disubtituted 1,2,3-triazoles. To PMA-Furf-coated NPs, Cy5.5-maleimide dye was attached by reacting the electron-rich diene of Furf with the electron-poor dienophile of Cy5.5-maleimide upon formation of cyclohexene derivative. Beside these strategies, the Fe_3O_4 PMA NPs were furthermore conjugated with amine-modified Dy-605 *via* EDC chemistry, in which EDC is used as a carboxyl activating agent to couple amines.

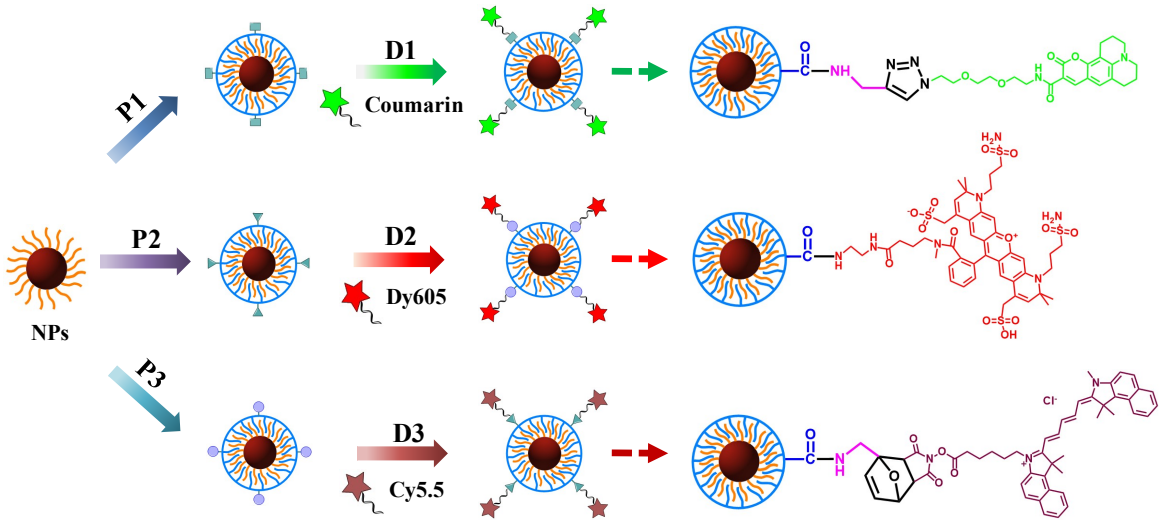

Figure 4. *Schematic illustration of the geometry of the used NPs. The surface modification of these NPs can be divided into two steps. Firstly, the NPs in organic solvent were transferred from organic solvent to water through polymer coating with three different derivatives of the amphiphilic polymer poly-(isobutylene-alt-maleic anhydride)-graft-dodecyl: PMA-Prop (P1), PMA (P2), and PMA-Furf (P3). Afterwards, they were functionalized with different dyes: Coumarin 343-azide (D1), Dy605-amine (D2), and Cy5.5-maleimide (D3). On the right, a sketch of the respective coupling chemistries is shown [71].*

The Fe_3O_4 NPs before and after the dye conjugated were compared using UV-Vis spectroscopy, Fluorometer, DLS, LDA, gel electrophoresis. Besides, quantification of dye conjugation (5-8 dye molecules per each NP) together with various detailed experimental procedures were also carried out, which can be found in the published paper [71].

3.4 Enzyme incubation and dye cleavage calculation

After the dye conjugation of Fe_3O_4 NPs, gel electrophoresis and ultracentrifugation were carried out for all NPs samples to remove the interferences of unbound dyes. In Figure 5, the experimental process to separate the cleaved dye with the modified NPs is demonstrated. The NP solutions were incubated with enzymes/enzyme mixture in PBS solution to the same volume for 24 h at 37 ℃: FBS (1%), trypsin (0.01%), CAT G (10 U/mL), LDH (10 U/mL), AST (5 U/L), ACHE (10 U/mL), and proteinase K (10 U/mL). After the incubation, the fluorescence intensity (I_0) of these samples were measured. As a next step, the samples were filtered with a centrifugal filter with a cut-off molecular weight at 100 kDa. During the centrifugation, small fragments from the polymer and dyes that cleaved by enzymes were eluted, and their fluorescence intensity marked as I_1. NPs that have larger molecular weight than 100 kDa were retained in the upper tube with filter membrane [71].

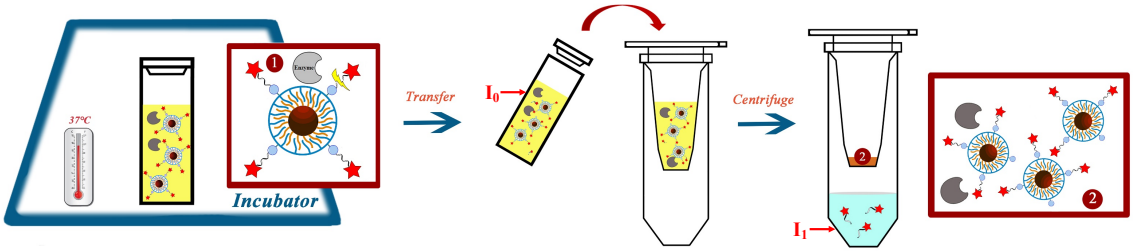

***Figure 5**. Measurement protocol for recording the fluorescence of the original NP solution (I_0) and the fluorescence of dyes/polymer fragments released from the NPs upon enzymatic cleavage (I_1) [71].*

Fluorescence intensity (I_0 and I_1) after enzyme incubation for 24 h can be found in Figure 6. From the fluorescence spectra, the dye emission intensity was determined at λ_{max}. Fluorescence intensity from enzymes without NPs was also measured as a control, which was negligible comparing with that from dye. After dye conjugation with NPs, a fluorescence quenching was observed due to re-absorbance of the NPs as reported by others [89]. Thus, after the enzymatic cleavage of dye from NPs, an enhancement of fluorescence intensity in I_0 was observed. I_1 came from the dissociated dye and fragments of PMA shell, which also proved the cleavage of dye. To check whether the fluorescence intensities of the lower part is due to leaking of intact NPs through the centrifuge filter or not, ICP-MS was used for the analysis and the result shows the amount of iron in the lower part was less

than 0.1% the mass of iron before centrifugation, confirming the degradation of the polymer shell. Meanwhile, the enzyme cleavage was also measured at different concentrations. An increase in the concentration of the enzyme will result in higher I_1, until a saturation concentration of enzymes is reached. No higher NP digestion could be achieved once the concentration of enzymes is saturated [71].

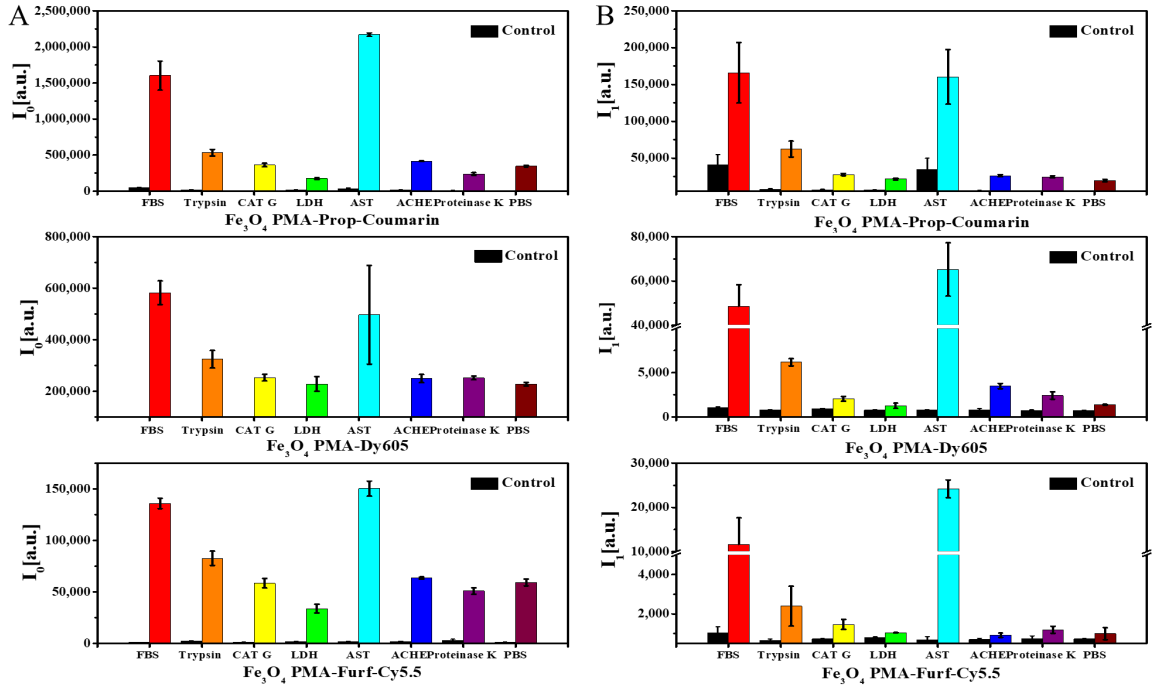

Figure 6. *(A) Mean emission intensities I_0 of NP solutions as incubated with enzyme mixes. (B) Mean emission intensities I_1 of small fragments of NPs which after enzymatic cleavage have been released from the NPs surface and which have been collected by ultrafiltration [71].*

To determine the dye dissociation from NPs quantitatively, the percentage of fluorescence from dye/polymer fragments cleaved from the NPs (I_1/I_0) (Figure 7 A) and the percentage of remaining fluorescence of the retained NPs ($(I_0-I_1)/I_0$) (Figure 7 B) are shown. Firstly, when enzymes are not added in the elutes (i.e. PBS only), I_1/I_0 value is minor, indicating that all dyes remained attached to the NPs. Meanwhile, as all dyes are attached either directly via amide bonds, or the linkers of the dyes are attached via amide bonds (as the polymer itself is composed out of dodecylamine chains linked to the polymer backbone by amide bonds), all enzymes which may cleave amide bonds (such as FBS, trypsin, CAT G and Proteinase K) can lead to degradation of the polymer shell. However, there are some examples for more selective cleavage based on the conjugation chemistries used for linking the dyes. In the presence of LDH, there was a high cleavage percentage

only in the case of Fe_3O_4 PMA-Prop-Coumarin NPs. On the other hand, AST predominantly acted on Fe_3O_4 PMA-Dy605 and Fe_3O_4 PMA-Furf-Cy5.5 NPs but not so much on Fe_3O_4 PMA-Prop-Coumarin. Thus, different enzymes may act on dyes as linked with different conjugation chemistries to the surface of NPs [71].

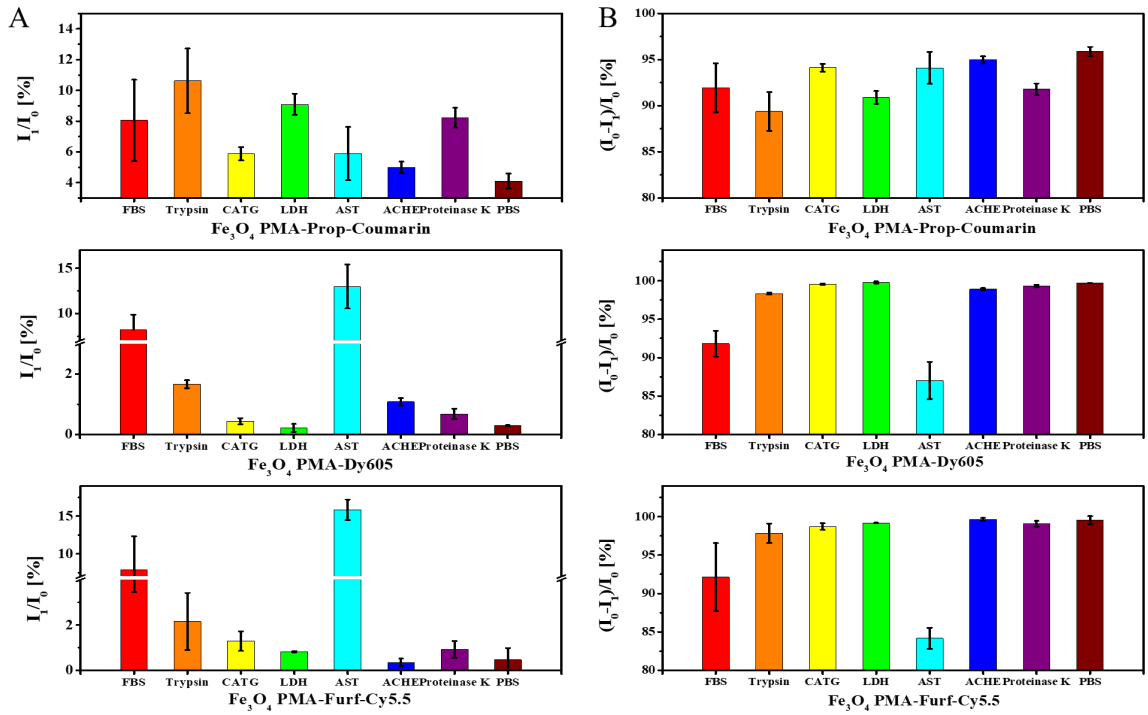

***Figure** 7. (A) I_1/I_0 and (B) $(I_0-I_1)/I_0$ of Fe_3O_4 PMA-Prop-Coumarin NPs, Fe_3O_4 PMA-Dy605 NPs, and Fe_3O_4 PMA-Furf-Cy5.5 NPs [71].*

Understanding the specific interactions between these enzymes and the NPs are arduous, even though different reaction mechanisms and enzyme-substrate intermediates are established [90, 91]. Except for the reaction specificities, enzymes were also reported to have promiscuity, where enzymes have functions in unexpected or unknown reactions [92]. In this enzyme incubation experiment, based on the results, we could reasonably speculate that LDH can cleave the bond that only exists in backbone of Fe_3O_4 PMA-Prop-Coumarin, and AST can catalyse the release of dyes in Fe_3O_4 PMA-Dy605 and Fe_3O_4 PMA-Furf-Cy5.5 through enzymatic degradation. However, more delicate investigations are needed in the future to reveal the detailed mechanisms. The dissociation of dye from the iron oxide NPs, which was confirmed by the fluorometer results, revealed the cleavage of organic polymer shell. In addition, different enzymes can lead to the break of different chemical bonds at various extents. This work helps us to collect more meaningful performances of

these enzymes, although understanding the detailed mechanism of such enzyme specific degradation still remains to be a great challenge due to the lack of corresponding background knowledge. More experimental knowledge about analogous enzyme functions is also of importance for directing future biological applications of NPs or some other biomolecules with similar chemical conjugations. For the applications of NPs at different biological environment with specific enzymes, it is suggested that the digestion of the polymer shell by these enzymes should be taken into consideration. Besides NPs, the enzyme degradation should be taken into account for any biomaterials with these bioconjugation strategies for their realization of designed in vivo use [71].

4. Au NCs

4.1 Motivation

When the size of the Au NCs comes to less than 3 nm (consisting of several to hundreds of Au atoms), they can obtain discrete energy level and size-dependent fluorescence as showed in figure 8. Bulk metals are electrical conductors due to the freely moving electrons in the conduction band. When the size decrease to ~3 to 100 nm, metal NPs have SPR phenomena by resonant oscillation of the conduction electrons in a continuous band structure after stimulated by light. In contrast, when metallic NCs have sizes comparable to the Fermi wavelength of the electron and the free electrons surrounding NCs decreased to a certain value, the NCs will have discrete energy level (HOMO-LUMO gap) induced by distinctive quantum confinement effects [93].

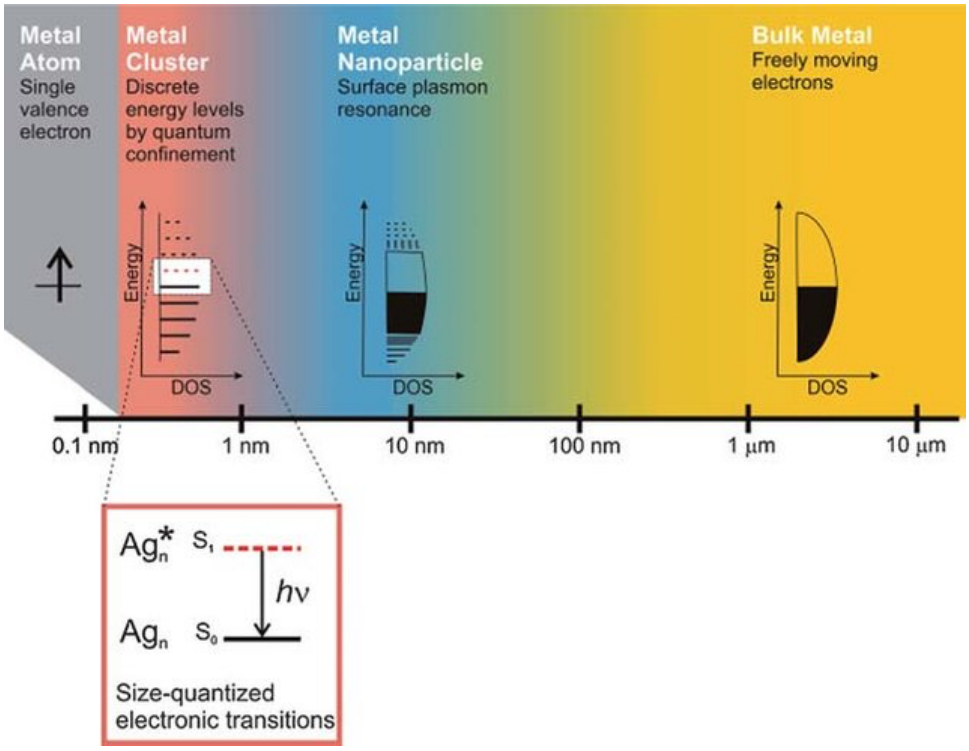

***Figure 8**. The effect of size on metals. Whereas bulk metal and metal NPs have a continuous band of energy levels, the limited number of atoms in metal NCs results in discrete energy levels, allowing interaction with light by electronic transitions between energy levels [94].*

As a kind of luminescent materials, NCs have long lifetime, large Stokes shift, and biocompatibility. Therefore, NCs can be used as good alternatives for biolabelling, imaging, detection and therapy. In general, organic dyes are always inferior to quantum dots due to the lack of good photostability. They suffer from rapid bleaching and are not bright enough in some applications. Quantum dots such as CdSe/ZnS NPs contain too many toxic elements and a high extent of cytotoxicity. Furthermore, quantum dots with the size ranging from 10 to 20 nm are too cumbersome as a fluorescence probe. For Au NCs, they can avoid the disadvantages of both organic dyes and semiconductor quantum dots. Especially, green synthesis of Au NCs (such as protein-stabilized Au NCs, enzyme-stabilized Au NCs) can avoid using toxic chemicals in the synthesis process and diminish the side-effects in biological applications [95].

To understand the photoluminescence origin of Au NCs is of huge importance for their future applications and have already attracted various attentions. Among them, except the particle size effects as widely referred to, other parameters such as ligands were also reported to influence the fluorescent properties [96]. For example, to investigate the role that ligands play in the fluorescence of the Au NCs, Zhikun et al. found that the covalent Au-S bond has a great effect on the electronic structure of Au NCs and results in the enhancement of fluorescence through the mechanism of LMCT [97]. The NCs with ligands that are more capable of pushing electron density to sulfur (or in another word, donating charges) or metal core with increased electropositivity (oxidation state) can have stronger fluorescence properties. However, there are also various controversial points, MLCT was also put forward to enhance the luminescence of Au NCs [98].

In this work, more efforts were dedicated into study the fluorescence properties of Au NCs by tailoring the various corresponding physico-chemical parameters, which is very meaningful to understand the mechanisms of NCs´ luminescence. Moreover, practical trials in this study could have reference functions to develop the design of high luminescent NCs.

4.2 In-situ synthesis of Au NCs

In this work, Au NCs were prepared by etching larger size Au NPs using 11-MUA in alkaline solution according to the protocol published by Huang [99]. As illustrated in figure 9 A, the Au NCs were prepared using ‘‘top-down’’ approach after the formation of Au NPs using ‘‘bottom-up’’ approach. In detail, the size of bigger Au NPs was around 2.9 ± 0.5 nm, and there were no apparent absorption and fluorescence of the as-synthesized Au NPs with the protecting ligand of THPC [99]. Then, these NPs were etched by 11-MUA to form smaller NCs with the size of 1.88 ± 0.18 nm by statistical analysis of TEM images. Figure 9 B demonstrated characteristics of Au NCs after synthesis, and they feature molecule-like absorption peak at 375 nm, emission peak at 510 nm and lifetime of 45 ns and 335 ns after fitting to a biexponential decay. The 11-MUA-Au NCs exhibit excellent fluorescence property with large Stokes shift (larger than 130 nm) and high luminescence. To monitor the formation of Au NCs, UV-Vis absorption spectra and fluorescence spectra by excitation at 375 nm were recorded during the in situ synthesis for 72 h, as shown in figure 9 C and 9 D. In the etching process, an absorption peak at 375 nm kept rising, which represents the increasing generation of Au NCs. Besides, a continuous increasing of the fluorescence intensity of Au NCs was also observed. The half time of the growth of Au NCs ($t_{1/2}$) was calculated by the sigmoidal fit of absorption and fluorescence intensity vs time, which were 31.0 ± 10.9 h and 26.2 ± 11.6 h respectively.

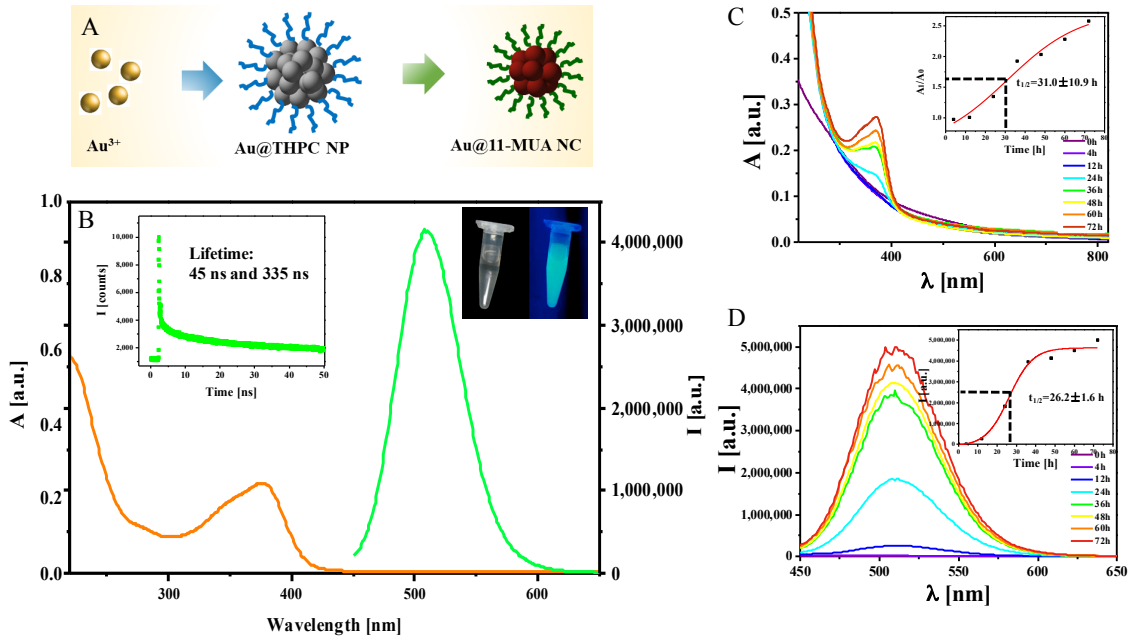

Figure 9. *(A) Schematic illustration for top-down and bottom up approaches for synthesis of Au NCs. (B) Absorption spectra (orange curve), fluorescence spectra (green curve), lifetime of Au NCs as well as their images both in normal and UV light. (C) UV-Vis absorption spectra and (D) fluorescence spectra as well as sigmoidal fit during the synthesis at different time point.*

4.3 Ligand conjugation of Au NCs

EDC chemistry was used to conjugate EDA and 3-ATPB to the surface of the Au NCs (the reaction scheme are in figure 10 A and 10 B). The conjugation of EDA and 3-ATPB were confirmed by the 1H proton NMR, and the proportion of 11-MUA ligands that have been conjugated is about 10% to 20%. After the reaction, these samples were cleaned by centrifugal filter to remove the excess ligands, and their UV-Vis absorption spectra, fluorescence spectra, zeta potential were recorded in Figure 10 C, D and E. From the UV-Vis absorption spectra, there were obvious transforms in absorption after binding with EDA and 3-ATPB, indicating the electronic structure changes in Au NCs. Especially for Au-3-ATPB NCs, a red shift (12 nm) and a broader absorption spectra were observed, which may be due to a slight increase of their size and a wider size distribution. There were a loss of luminescence of Au-3-ATPB NCs and a sharp fluorescence reduction in Au-EDA NCs. The conjugation with EDA and 3-ATPB also resulted in a decrease of zeta potential value.

In alkaline solution, Au NCs with ligands of 11-MUA have negative charge due to the carboxylic group. However, when a part of the carboxylic group was bonded, the zeta potential of these NCs can be less negative. Additionally, Au-EDA NCs have the least negative charge due to the presence of amino chain after the conjugation, which can be protonated (NH_3^+). Figure 10 F, G and H showed the excitation-emission spectra of Au NCs, Au-EDA NCs and Au-3-ATPB NCs, in which the blue shift in fluorescence of samples after ligand conjugation was observed in contrast to Au NCs. And the images of each sample under UV light also affirmed the decrease of fluorescence intensity after ligand conjugation. Combing the UV-Vis absorption spectra, the fluorescence quenching can be elucidated due to structural distortion and different optical absorption that caused by charge anisotropy [100]. Also, by speculation according to mechanism of LMCT, after electron-withdrawing carboxylic group was conjugated, the electron donation capability of ligand to metal core would be subsided and fluorescence quenching occur.

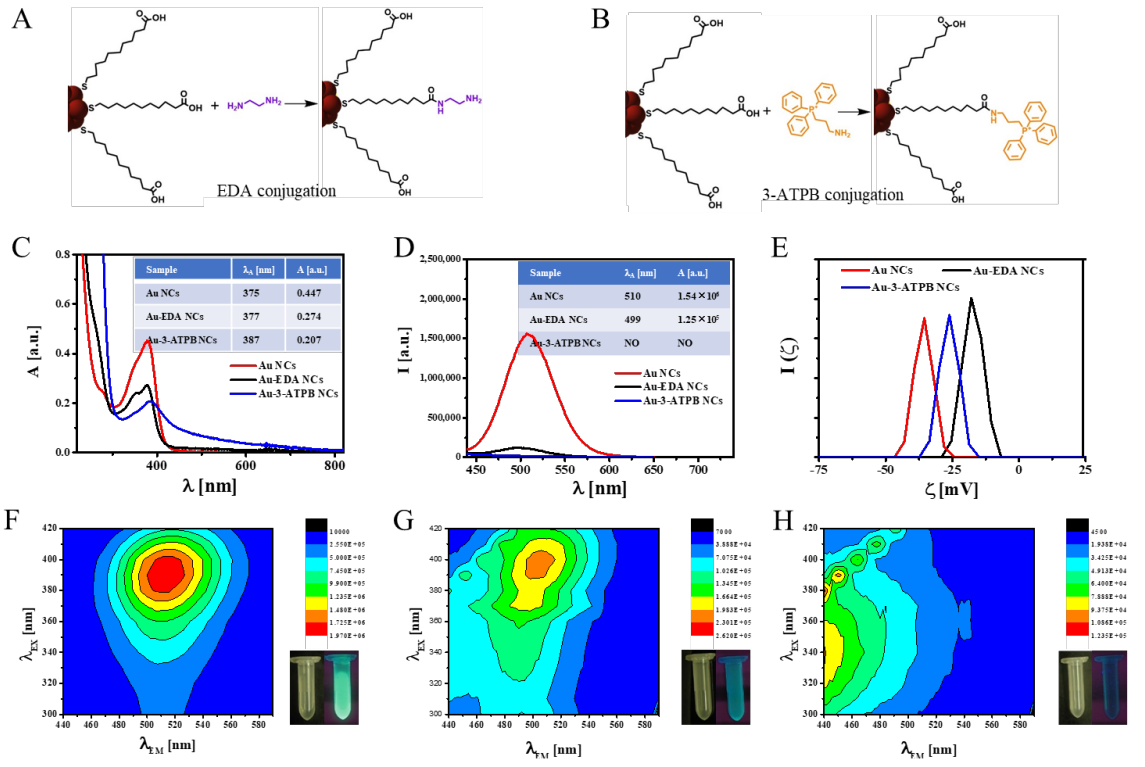

Figure 10. *Reaction scheme between 11-MUA at the surface of Au NCs and (A) EDC as well as (B) 3-ATPB; (C) UV-Vis absorption spectra, (D) fluorescence spectra and (E) zeta potential of Au NCs before and after conjugation; Excitation-emission matrix spectra of (F) Au NCs, (G) Au-EDA NCs and (H) Au-3-ATPB NCs.*

4.4 Effect of metal ion on Au NCs

The fluorescence properties of NCs can also be altered after reaction with metal ion, and the detection copper and mercury ion by NCs is on account of this phenomenon [101]. In this part of our work, different metal ions such as Ag^{+}, Pd^{2+} and Pt^{4+} were incubated with Au NCs at different concentrations. The schematic diagram in figure 11 A demonstrated the possible principle of interaction between NCs and metal ion. As is known to all, the metal exchange is generated by galvanic replacement reactions between active metal NP with more noble metal ions. However, metal exchange for the ultrasmall NCs and metal ion seem to not follow the classical metal activity sequence (Ag＞Pd＞Pt＞Au). As reported by Wang, the metal exchange of inert Au NCs with Ag^{+} does not follow the metal activity sequence, and the doping silver atoms can be re-exchanged by Au^{+}, which is related with the electron shell closing and the structural stability [102]. In our experiments, UV-Vis absorption spectra and fluorescence spectra after metal exchange of Au NCs with Ag^{+} at concentration from 1 mM to 25 mM were illustrated in figure 11 C and 11 D. With the increase of Ag^{+} concentration, the absorption declined at 375 nm and climbed at 340 nm, indicating the alternation of the electronic structure. The fluorescence intensity was also decreased with rising Ag^{+} concentration. In another incubation experiment using $AgNO_3$ instead of AgCl, similar results were obtained. These results also confirmed the metal exchange between Au NCs and Ag^{+} in our case. For the Pd^{2+} and Pt^{4+}, the fluorescence quenching also occurred at different extents as illustrated in 11 B. However, from their UV-Vis absorption spectra after incubation with Pd^{2+} and Pt^{4+} that would be demonstrated later, there was only an overall rise in absorption spectra without huge changes, which may indicate the general maintenance of NCs´ structure. The absorption spectra transforms were really similar to oxidation-like changes as that in next section 4.5. Thus, for the incubation with Pd^{2+} and Pt^{4+}, the metal exchange process was not verified yet and their fluorescence change may due to the redox process [103]. However, the replacement of other atom (Pd and Pt) to the Au NCs core seem to be not valid except Ag atom, which may because of the size match of Ag and Au (below 1% distinction) and therefore Ag atom is more capable for binding to Au NCs core. [104].

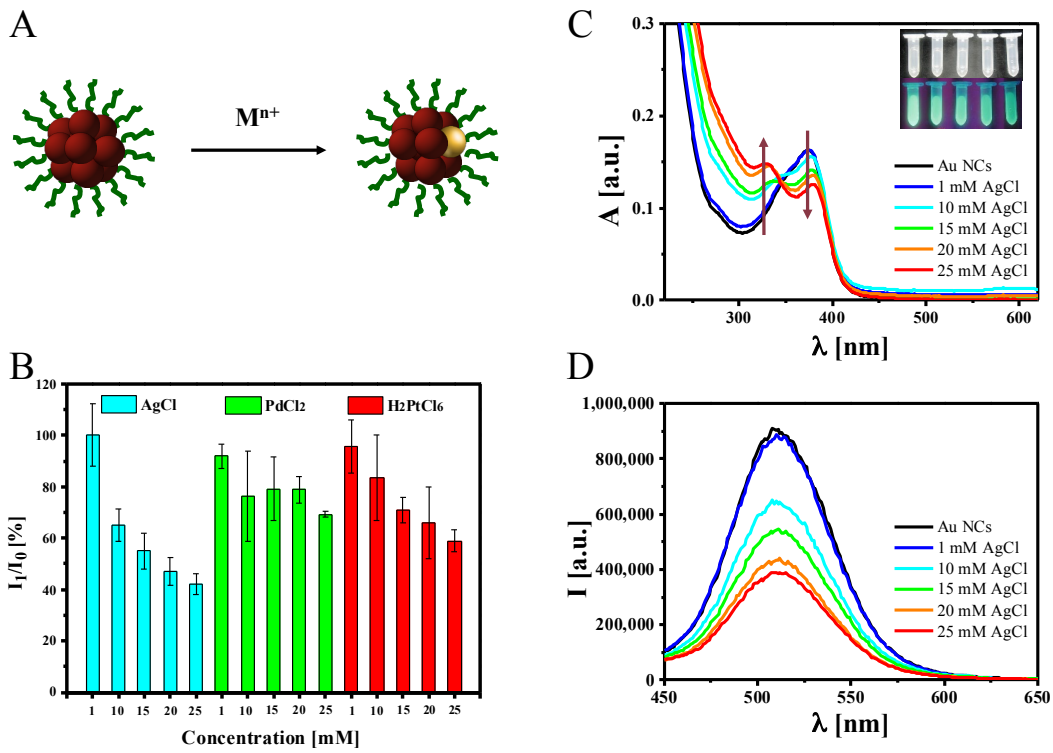

Figure 11. *(A) Schematic representation of metal exchange. (B) The I_1/I_0 value dependent on different concentration of metal salts (I_1 represents sample´s fluorescence intensity after incubation with metal salts, I_0 represents Au NC´s original fluorescence intensity). (C) UV-Vis absorption spectra and (D) fluorescence spectra of Au NCs at different concentrations.*

4.5 Redox reaction of Au NCs

Au NCs can adopt different valence state, and their valence state was found to influence on the properties of Au NCs, such as LMCT effects. According to this theory, the increase of electropositivity of the metal core leading to the strength of charge transfer from the ligand to the core and result in fluorescence enhancement. As reported by Jin, $[Au_{25}(SR)_{18}]^-$ NCs can be oxidized to higher charge and higher oxidation state leads to stronger fluorescence [97]. However, the mechanism of how it affects the photoluminescence of NCs is still elusive.

In our study, oxidation of 11-MUA coated Au NCs was performed by using H_2O_2, which is one of the most powerful oxidizer. Afterwards, UV-Vis absorption spectra as well as fluorescence spectra were collected with time in figure 12 B and 12 C separately. After the

oxidation, the absorption peak ascended to higher intensity with a rise of baseline, and the shape of absorption seems to be similar with that before oxidation. The fluorescence intensity decreased dramatically in figure 12 C, and the blue shift of emission wavelength was observed obviously in excitation-emission matrix spectra, which will be exhibited later. According to LMCT, the oxidation effects may lead to increasing valence state of Au that can lead to fluorescence enhancement, which is to the contrary of our results. In our speculation, as the presence of H_2O_2, oxidation can also result in oxidation of 11-MUA to form organic disulfide product, which resulted in fewer ligands that are bound the surface of Au NCs as illustrated in figure 12 A [105]. The loss of capping ligands can also be the reason for reduced luminescence.

In figure 12 D and 12 E, the UV-Vis absorption spectra and fluorescence spectra after reduction by $NaBH_4$ were measurements at different time point. The absorption and fluorescence intensity after reduction were decreased gradually. After 2 h, the absorption peak of the sample turned from 375 nm to around 510 nm, which may be caused by the formation of Au NPs. The colour of the sample after reduction for 2 h has changed to red, which also indication the generation of Au NPs. As the increase of the size, the electronic structure of these samples will be significantly changed, and their luminescence finally vanished. According to our conjecture, the addition of reducing agent can result in the generation of Au(0) around Au NCs, and Au NCs finally grew into Au NPs with bigger size, as displayed in 12 A.

In total, Au NCs have the highest luminescence with the stable oxidation state after synthesis. Oxidation and reduction will change the valence state or size of NCs, and they will cause the loss of fluorescence.

Apart from these measurements, some other trials such as ligand exchange with ligands at n-alkanethiolates family with different carbon length were performed, and there was no obvious difference in fluorescence among samples after ligand exchange. This result may indicate the insensitivity of Au NCs in the ligand carbon length and the ligand effects may not so play the dominant role in fluorescence of Au NCs.

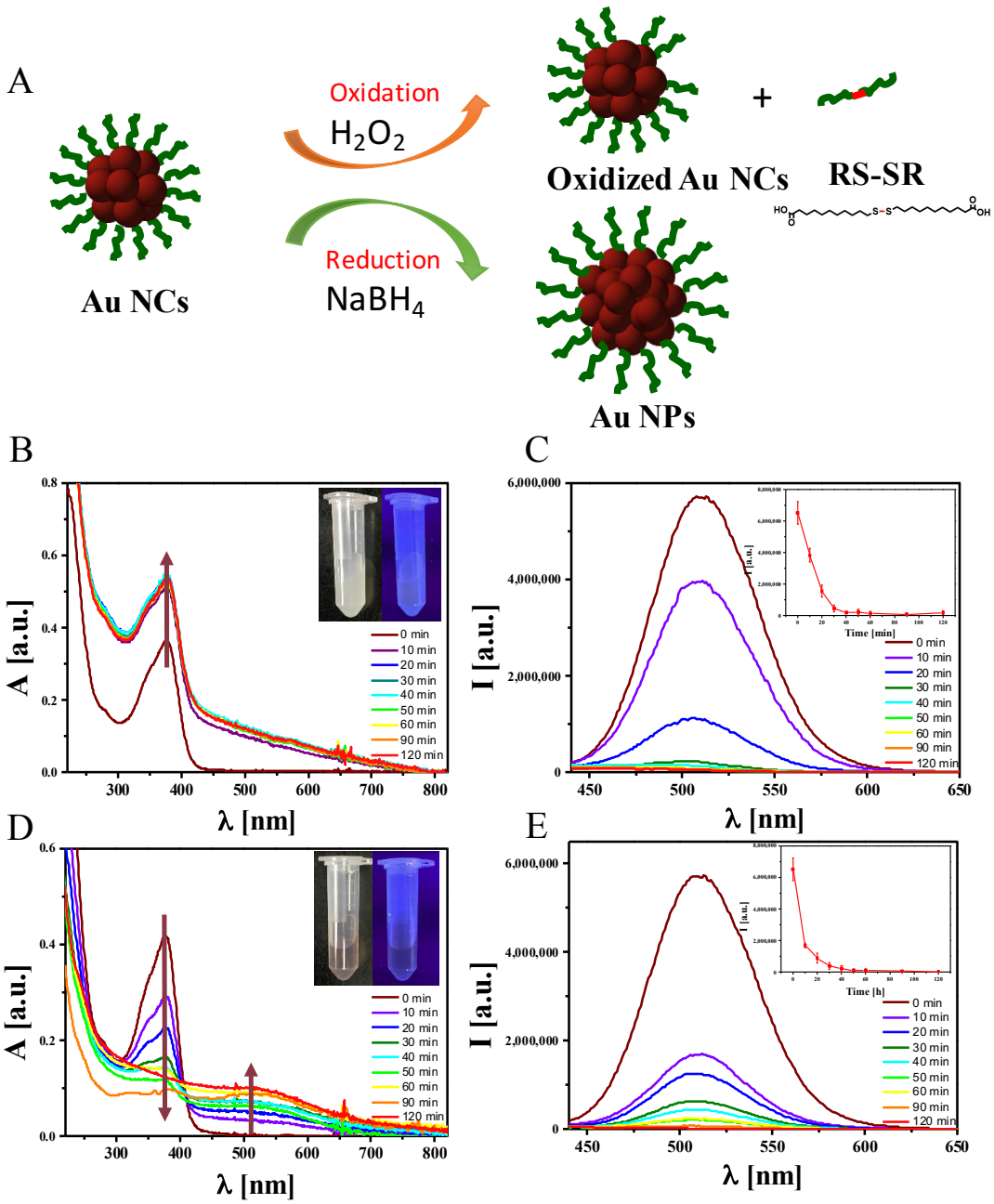

Figure 12. (*A) Schematic representation of redox reaction of Au NCs. (B) UV-Vis absorption spectra as well as sample images under normal and UV-light after oxidation with H_2O_2 for 2 h. (C) fluorescence spectra of Au NCs and the curve of fluorescence intensity vs time after oxidation by H_2O_2. (D) UV-Vis absorption spectra as well as sample images under normal and UV-light after reduction with $NaBH_4$ for 2 h. (E) fluorescence spectra of Au NCs and the curve of fluorescence intensity vs time after reduction by $NaBH_4$.*

5. Ag NCs

5.1 Motivation

In addition to Au NCs, Ag NCs also have extraordinary molecule-like properties due to their size, exhibiting photoluminescence but not plasmatic properties. The research on Ag NCs is also focused on their photoluminescence. According to various studies, Ag NCs even showed brighter fluorescence than Au NCs in solution, which is also have great potential in application for biosensing and bioimaging [106].

For Ag NCs, how the core or ligand surface of NCs impact on the luminescence seems to be also debatable. Ag-carboxylate NCs is suggested to have the fluorescence through LMCT mechanism, by which electron transferring from the oxygen atom in the carboxylate ligands to the Ag core [107]. The interplay between ligands and core were also taken into account and extended the superatom model by Walter in 2008 [108]. Ligands were perceived to affect the electronic structures and optical properties of NCs, and additional ligand band orbitals. However, a latest study on fluorescence on NCs have the viewpoint that fundamental origin of photoluminescence is in kernel emission as showed in figure 13 [109]. This study confirmed that the origin of fluorescence lies in kernel-dominated LUMO to HOMO transition, and the surface vibration can affect quantum yield of NCs. Apart from this dispute, various other factors may also effects on fluorescence. For example, a research with 10 % to 40 % Au-doped Ag NCs (prepared by reduction of mixture of Ag and Au metal precursor at different proportion) found a strong enhancement of photoluminescence and stability [110].

In our study, the origin of photoluminescence from Ag NCs was also studied to have a thorough understanding of their properties for biosensing application. The atomically precise $Ag_{29}(DHLA)_{12}$ NCs were chosen in this research with obvious characteristic absorption bands. Except metal exchange, ligand exchange, ligand conjugation and oxidation experiments, the phase transfer of Ag NCs from water to organic solvent were also investigated to gain more insight into their photoluminescence property.

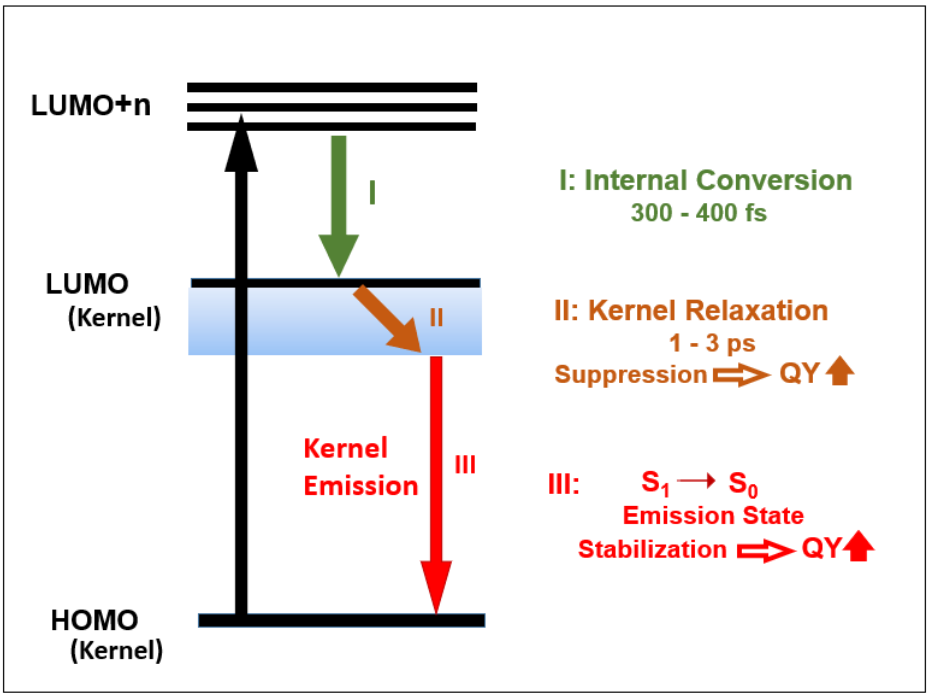

Figure 13. *Kernel-emission model that summarizes relaxation diagram and time-constants obtained from transient absorption measurements [109].*

5.2 In-situ synthesis of Ag NCs

To synthesis $Ag_{29}(DHLA)_{12}$ NCs, bottom up and top-down approaches were performed in a single experiment within 5 h [111]. The characteristics of Au NCs were exhibited at figure 14 A. From the UV-Vis absorption spectra and fluorescence spectra in figure 14 B and figure 14 C, the growth process and generation of fluorescence were clearly monitored. At the first stage of synthesis, a broad plasmonic peak at 460 nm was caused by the bigger NPs, which is the bottom-up approach during synthesis. In the following time, these bigger NPs can break into smaller NCs spontaneously, and afterwards another characteristic absorption curve would start appearing, which has three intense bands at 320, 425 and 500 nm. After the formation of Ag NPs, fluorescence intensity was about neglectable, and then there was a dramatic increase of fluorescence intensity with formation of Ag NCs. The synthesis of Ag NCs took about 4.5 h, and a sigmoidal (Boltzman) fit were used to calculate the half time of the NCs´ synthesis ($t_{1/2}$=2.05±0.6 h). After the synthesis, some other information of Ag NCs were also collected such as TEM image, hydrodynamic diameter and zeta potential.

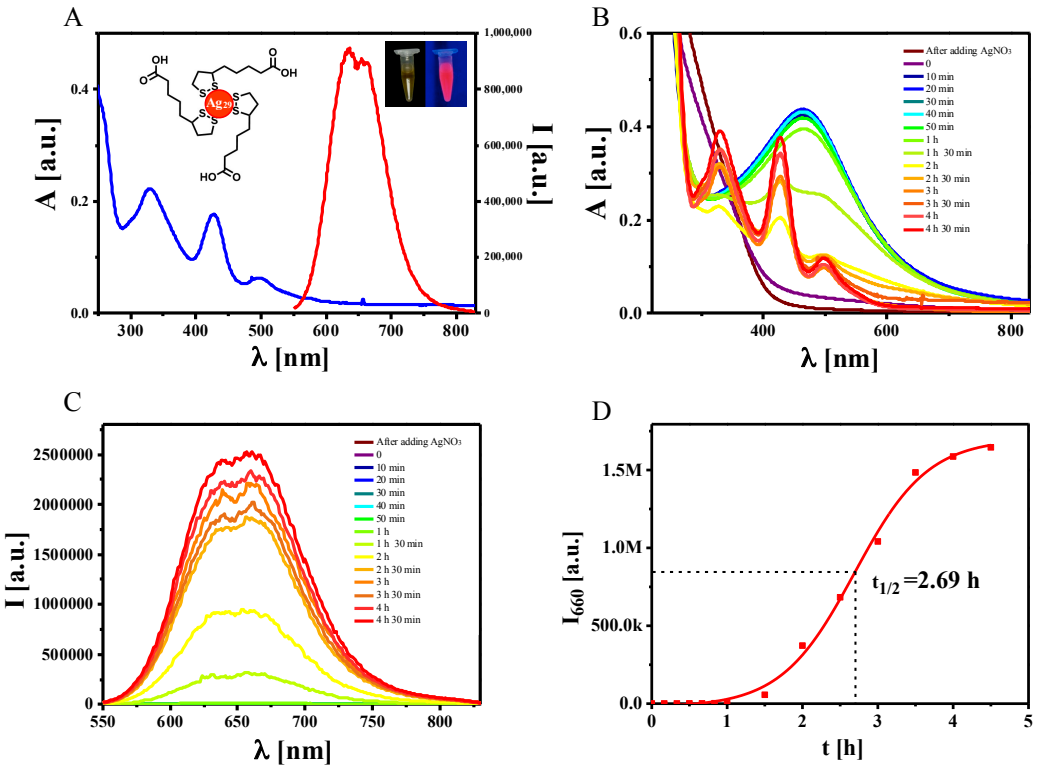

Figure 14. *(A) Absorption (blue curve), fluorescence spectra (red curve), chemical structure of Ag NCs as well as their images both in normal and UV light. (B) Absorption spectra and (C) fluorescence spectra during in-situ growth of Ag NCs. (D) Fluorescence intensity versus time of the synthesis to calculate the* $t_{1/2}$ *for the synthesis.*

5.3 Metal exchange of Ag NCs

Various bimetallic NCs have been prepared by the core metal galvanic exchange reaction between metal NCs and salts of more noble metal. With the formation of bimetallic NCs, they have different performance in fluorescence due to different composition of core and may also cause the structure transformation. For example, Ag/Au NCs were belong to one of the most frequently studied bimetallic NCs. Also, by control the Ag/Au molar ratios, the luminescence of the alloy NCs was adjustable from visible red to NIR [112]. Some trials by one-pot synthesis of bimetallic NCs were also feasible, like the Pt growth in Ag/Pt NCs were initiated by the galvanic replacement reaction after the formation of Ag NCs [113]. In these studies, fluorescence enhancement and quenching were both discovered.

In the experiments with $Ag_{29}(DHLA)_{12}$ NCs, the metal salts of $AuCl_3$, $HAuCl_4$, $PdCl_2$ and H_2PtCl_6 were incubated with the as-synthesized Ag NCs with the final metal salts concentration at 1 mM, 10 mM, 15 mM, 20 mM and 25 mM. The absorption spectra of Ag NCs after incubation were recorded in figure 15 A, B, C and D separately. In all samples, the UV-Vis absorption of 3 intense bands got less sharp. The samples incubated $AuCl_3$ and $HAuCl_4$, which were exactly reacted with same metal ion, went through similar transformation process. Alternation of optical spectra are attributed to the electronic structure conversion that may cause by structural change. Besides, these changes also affirm the replacement of Ag by other metals. In figure 15 E, I_1/I_0 value represents how much the fluorescence intensity has been altered. Due to the increase of the metal concentration, the quenching effects were raising and the finally fluorescence intensity decreased to a very low level.

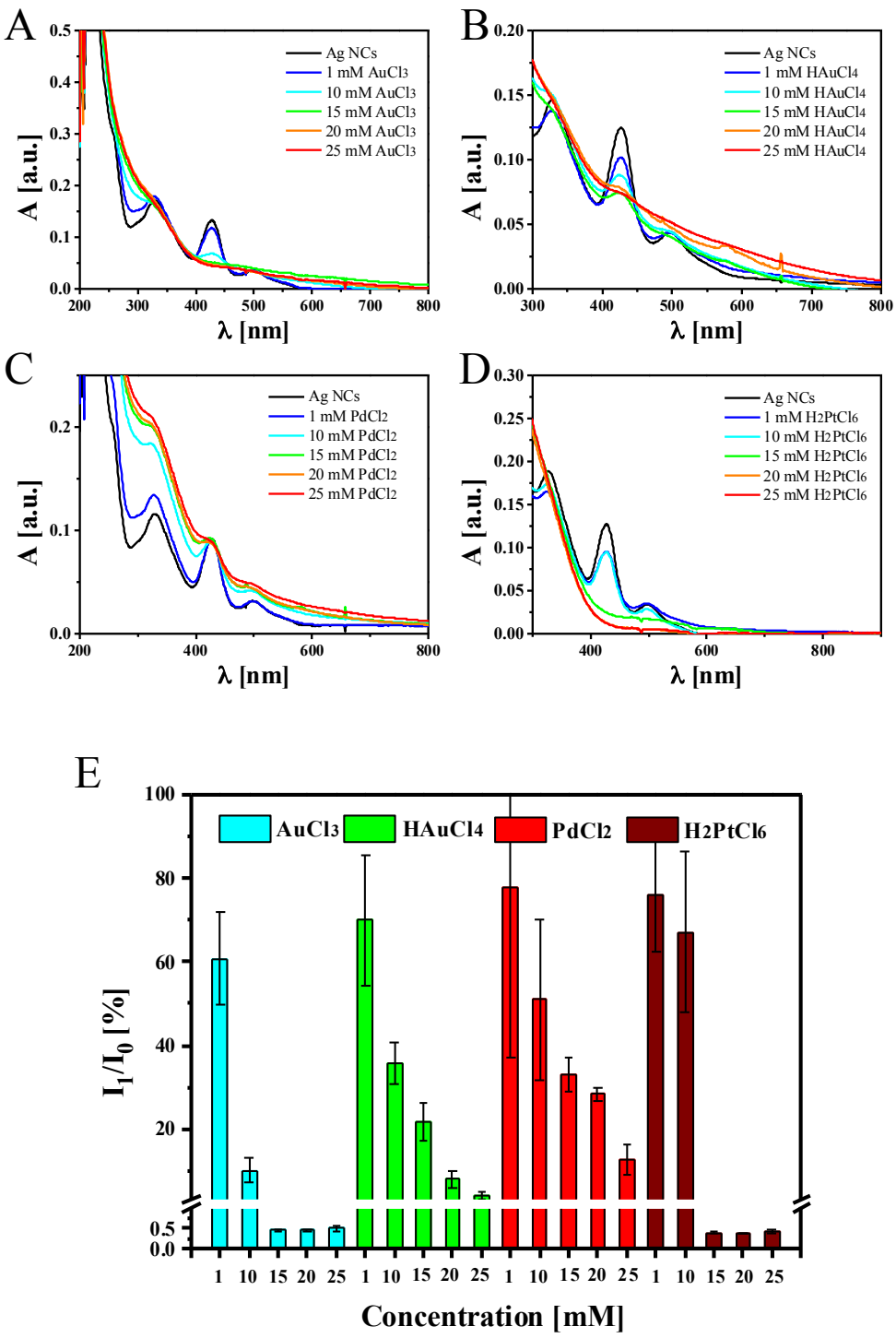

Figure 15. *Concentration dependent UV-Vis absorption of Ag NCs after incubation with (A) $AuCl_3$, (B) $HAuCl_4$, (C) $PdCl_2$, and (D) H_2PtCl_6. (E) The I_1/I_0 value dependent on metal salts at different concentration (I_1 represents sample´s fluorescence intensity after incubation with metal salts, I_0 represents Au NC´s original fluorescence intensity).*

5.4 The effect of ligand length on the fluorescence of Ag NCs

To research the role of ligands in the fluorescence of the Ag NCs, a series of ligand exchange experiments were performed with the ligands from same n-alkanethiolates family with increasing carbon chain length, such as TGA, 3-MPA, 6-MHA, 8-MOA, 11-MUA. From figure 16 A B and C, by changing the n-alkanethiolates ligands, the physical properties of the Ag NCs including the absorption, fluorescence intensity and zeta potential were different while the surface chemistry should be analogous. After ligand exchange with these ligands, the shape of absorption spectra was largely changed. Especially the sample with 11-MUA, there was only a shape peak at around 340 nm. The huge diversity of absorption spectra may indicate the alternation of their structure after ligand exchange. Besides, with the increase of carbon chain length, the fluorescence intensity decline sharply, although the emission peak positions were similar. Some proposed mechanisms may also be used for explanation, such as LMCT effects. The carboxylic group is electron-withdrawing group that can possibly directly donate electron to the metal core, but these effects can be reduced if the carbon chain increased to be long enough, leading to the fluorescence quenching. And the emission wavelength of Ag NCs maintained after ligand exchange, which is in accord with the model with the kernel-dominated LUMO to HOMO transition [109].

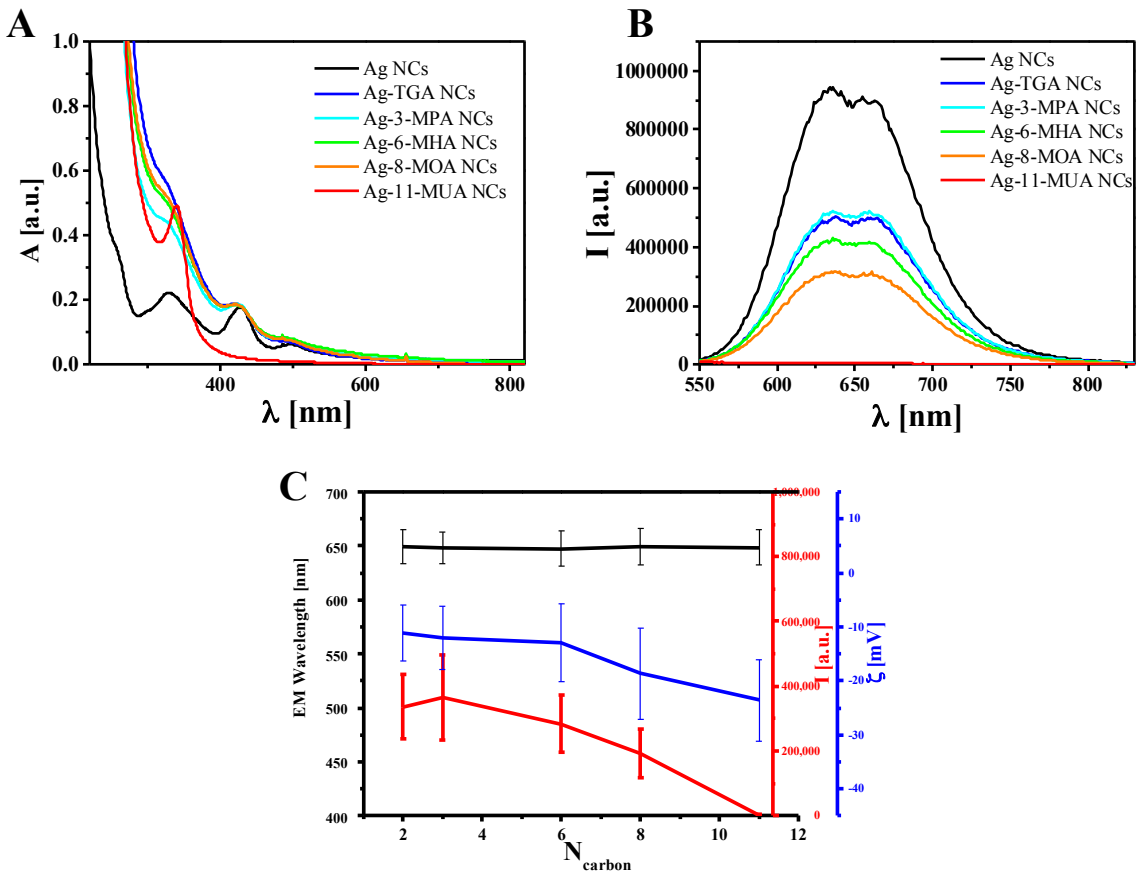

Figure 16. *(A) UV-Vis absorption spectra and (B) fluorescence spectra of samples after ligand exchange with TGA, 3-MPA, 6-MHA, 8-MOA and 11-MUA. (C) Plot of emission wavelength, emission intensity and zeta potential with carbon length of different ligands.*

5.5 Phase transfer of Ag NCs

The as-synthesized Ag NCs dissolved in water were mixed with the same volume of toluene on the use of serials of capping ligands such as TOAB, THPC, TPPB, TPAB and CTAB with gentle stirring. After these trials in 2 h, pics of these samples were taken under normal and UV light as showed in figure 17 A. As can been seen, only the one with TOAB that can result in the phase transfer from water to TOAB. The phase transfer occurred by the electronic attraction between hydrophilic carboxylate anion of the DHLA ligand and hydrophobic tetraoctylammonium cation in toluene. By comparing the absorption spectra and fluorescence spectra of Ag NCs before and after phase transfer in figure 17 B and C, the enhancement of both absorption and fluorescence intensity is observed. From the UV-

Vis absorption, the absorption spectra after phase transfer is found to be similar with that before phase transfer. The peak at 320 nm and 425 shifted about 5 nm to higher wavelength, and the peak at 500 nm shifted gently to lower wavelength. Thus, the Ag NCs seems to be in a narrower size distribution and there was a gentle deformation in the electronic structure after phase transfer reaction. From the fluorescence spectra, after the phase transfer, the fluorescence intensity was enhanced and a blue shift of the fluorescence can be seen. The emission wavelength change can be resulted of the kernel transformation. Besides, with data analysis in parallel samples, the fluorescence intensity of Au NCs in toluene increased 17.5±7.2 % at 650 nm compared with that in water, which may also due to the increased integrity after phase transfer.

In addition to these investigations, $Ag_{29}(DHLA)_{12}$ NCs were also found to have reversible fluorescence after oxidation by H_2O_2 and reduction by $NaBH_4$, which indicate the reversible chemical process of cluster formation and degradation [114].

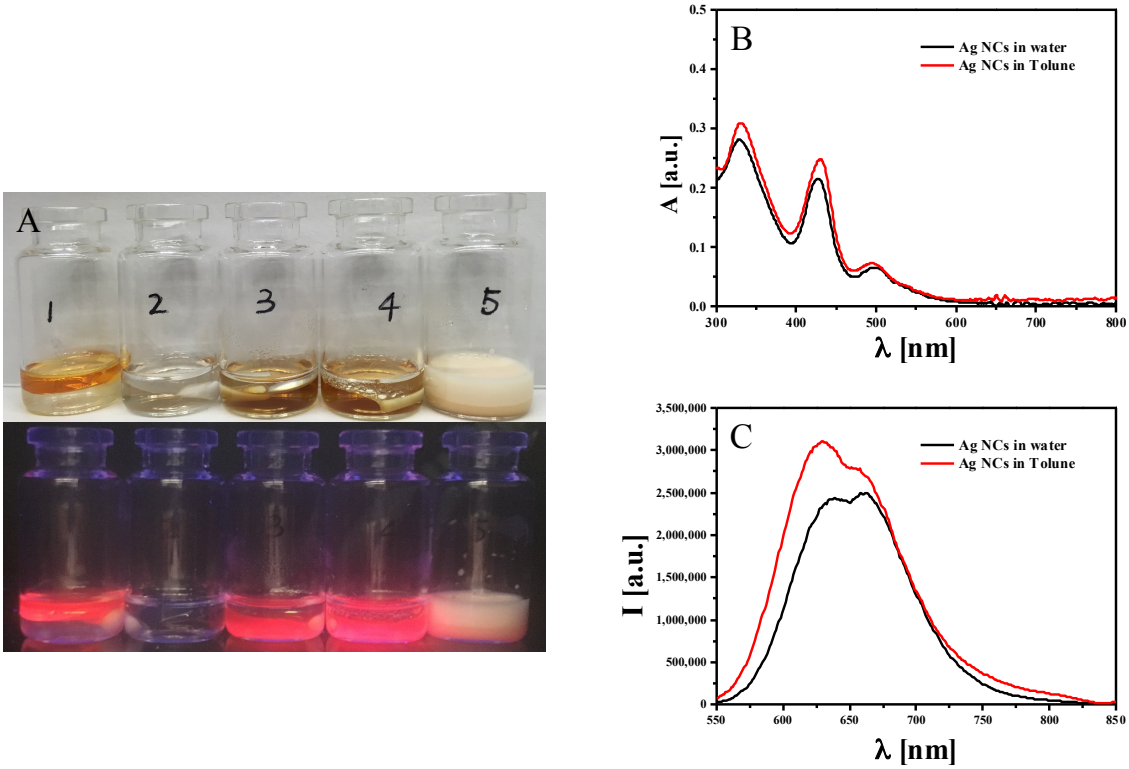

Figure 17. *(A)Images of trials of phase transfer with the surfactants of TOAB, THPC, TPPB, TPAB and CTAB (left to right) under normal and UV light. (B) UV-Vis spectra and (C) fluorescence spectra of Ag NCs in water and in toluene.*

6. Conclusion and outlook

In this work, iron oxide NPs, Au NCs and Ag NCs were synthesized and investigated to advance their future biological applications. For iron oxide NPs, former studies indicate their prospects for diverse usage: magnetic separation of specific biological entities after labelling, drug carrier to target sites using an external magnetic field, hyperthermia therapy to treat cancer and MRI contrast enhancement. Thanks to the fluorescent properties of Au NCs and Ag NCs, they are promising nanomaterials for biosensing, biolabeling and bioimaging. Specifically, they were recommended for detection of small biomacromolecules (such as cysteine, glutathione and dopamine), specific probing when labeled with cells and cancer diagnosis through microscopy imaging [115]. The works depicted in this thesis enhance our knowledge to improve the performances of NPs and NCs for their future applications.

For the work with Fe_3O_4 NPs, the separation of dye from the surface of NP is due to enzymatic degradation on polymer shell around inorganic NP core. By the measurement of their fluorescence intensity, the degradation extents of various enzymes can be quantified. The results indicate that degradation depends on the types of enzymes the NPs encounter, as well as the conjugation chemistry with which dyes are linked to the polymer shell. Concerning use of the NPs in biological scenarios, enzymes thus always should take into account. As enzymatic digestion of the NPs, surface coating may significantly vary the functional and physico-chemical properties of the NPs. In addition, this enzymatic degradation must be considered specially when analysing the performance of biomolecules (i.e., antibodies, antifouling agents, drugs, carbohydrates, etc.) bound to the NP´s surface using any of these bio-conjugation strategies.

For Au NCs, various investigations such as ligand conjugation, metal ion and redox reactions were implemented to check their effects on Au NCs´ fluorescence. A blue shift and a sharp decline were witnessed in fluorescence emission after conjugation with EDA, and the fluorescence property was completely out of action after conjugation with 3-ATPB. These changes were due to the structural distortion or ligand conjugation with carboxylic group, which is a good electron donating group. The incubation between Au NCs and metal ion (Ag^+, Pd^{2+} and Pt^{4+}) eventually result in the fluorescence quenching at different extents,

in which metal exchange occurred with Ag^{+} and the reactions of Au NCs with Pd^{2+} and Pt^{4+} may be only considered as redox process. Finally, both oxidation and reduction reaction will alter the fluorescence property of Au NCs, causing the decrease of luminescence by removing of capping ligands and size increase.

The study of Ag NCs was also focused on their fluorescence behavior under measurements of metal exchange, ligand exchange, and phase transfer. The metal exchange of Ag NCs took place with Au^{3+}, Pd^{2+} and Pt^{4+}, causing the fluorescence quenching similar with that in Au NCs. After ligand exchange with n-alkanethiolates ligands at different carbon length, the fluorescence intensity was decrease with carbon length of ligands because of LMCT effect. In the final phase transfer experiment, the enhancement of fluorescence and blue shift in emission can be seen. This result elucidate the kernel transformation and improved stability after phase transfer. In these studies, control of luminescence by changing various physico-chemical parameters were achieved, which are significant for the design of high luminescent NCs.

In this thesis, the studies with different goals were achieved for improving application of nanomaterials in biological circumstances. On one hand, some newly invented nanomaterial are still with mystery, which may need scientists to disclose their features. On the other hand, to use varieties of novel nanomaterials safely, more in vivo and in vitro measurements with biological components are essential. In the future decades, more and more nanomaterials will come into use for life science applications.

Abbreviations

NP	nanoparticle
NC	nanocluster
Au	gold
Ag	silver
TEM	transmission electron microscope
AFM	atomic force microscopy
NMR	nuclear magnetic resonance
IR	infrared
CdSe	cadmium selenide
CdS	cadmium sulfide
NIR	near infrared
Fe_3O_4	ferrous ferric oxide
FePt	Iron platinum
CVD	chemical vapor deposition
NaCl	sodium chloride
He	helium
Ar	argon
Si	silicon
Cu	magnetic resonance imaging
Pt	nanoparticle(s)
Pd	Octylphosphonic acid
NaBH4	sodium borohydride
DNA	Deoxyribonucleic acid
MRI	magnetic resonance imaging
PLGA	poly (S,L-lactide-co-glycolide)

Ag_2S	silver sulfide
FT-IR	Fourier-transform infrared spectroscopy
ROS	reactive oxygen species
ZnO	zinc oxide
UV-Vis	ultraviolet–visible
DLS	dynamic light scattering
LDA	laser doppler anemometer
ICP-MS	Inductively coupled plasma mass spectrometry
EDC	1-Ethyl-3-(3-dimethylaminopropyl)carbodiimide
PMA	poly-(isobutylene-alt-maleic anhydride)-graft-dodecyl
SPION	superparamagnetic iron oxide nanoparticles
CuAAC	Cu(I)-catalyzed azide-alkyne cycloaddition
Prop	propargylamine
Furf	Furfurylamine
PBS	phosphate buffered saline
FBS	fetal bovine serum
CAT G	cathepsin G
LDH	lactate dehydrogenase
AST	aminotransferase
ACHE	acetylcholinesterase
SPR	surface plasmon resonance
11-MUA	11-mercaptoundecanoic acid
THPC	tetrakis(hydroxymethyl)phosphonium chloride
EDA	Ethylenediamine
3-ATPB	3-(aminopropyl)triphenylphosphonium bromide

LMCT	ligand to metal charge transfer
MLCT	metal to ligand charge transfer
H_2O_2	hydrogen peroxide
ZnS	zinc sulfide
DHLA	dihydro lipoic acid
$AuCl_3$	gold(III) chloride
$HAuCl_4$	hydrogen tetrachloroaurate(III) trihydrate
$PdCl_2$	palladium(II) chloride
H_2PtCl_6	chloroplatinic acid hexahydrate
TGA	thioglycolic acid
3-MPA	3-Mercaptopropionic acid
6-MHA	6-mercaptohexanoic acid
8-MOA	8-mercaptooctanoic acid
TOAB	tetraoctylammonium bromide
THPC	tetrakis hydroxymethyl phosphonium chloride
TPPB	tetraphenylphosphonium bromide
TPAB	tetrapropylammonium bromide
CTAB	hexadecyltrimethylammonium bromide

Acknowledgements

In September 2015, I started my Ph.D. study in Marburg. In 2019, I am about to finish my Ph.D. study in Hamburg. The four years are filled with memories that are precious treasures to me.

First of all, I would like to express my sincere appreciation to my supervisor Prof. Wolfgang Parak for all his guidance and support during my study. He brings me to the world of nanoparticles and provides me a good opportunity for working in such an interesting field. Prof. Wolfgang Parak has all the qualities as a scientist, always passionately and effectively in scientific research, intelligent and confident. I am honoured that I could have the chance to see how a great mind works.

My sincere thanks also goes to Dr. Indranath Chakraborty for his continuous support during my Ph.D. study. He has a serious attitude to work. This work cannot be conducted without his guidance and the numerous constructive and stimulating discussions that we have had. Thanks for all the time he has spent in helping me, which makes me become a more professional researcher.

I am also very grateful to Dr. Beatriz Pelaz Garcia for her advices in the first year of my PhD study. Her patient teaching of experimental operation and explanation of fundamental theoretical in nanoparticles. Without her support in the first year, I could not have learned so fast and gained a good understanding of my work.

The help from all my colleagues at University of Hamburg is also greatly appreciated. Thanks to Dr. Neus Feliu for her kindness and patience in all the discussion and answering me related questions; Dr. Dingcheng Zhu for his help in NMR measurements, analysis and all the other technical problems; Prof. Dr. Alaaldin M Alkilany for all the enlightening suggestion due to a wealth of his knowledge; all the other members of our group to have a very pleasant and helpful environment.

I am also grateful to the staff members in University of Hamburg. For the laboratory maintenance, I am very thankful to Marten Rittner for ordering all the laboratory supplies and repairing instrument fault and Petra Roth for all the file processing.

Thanks to China Scholarship Council (CSC) for the financial support during my study.

I would like to take the chance to thank my family and friends for their understanding, emotional support and unconditional love. I would also like to thank myself for everything I have done to be a better person, being adaptable to the foreign environment, being strong during hard times, being humble when I made achievements, and being satiable in life.

Hamburg, in April 2019 Lin Zhu

References

[1] A.K. Gupta, M. Gupta, Synthesis and surface engineering of iron oxide nanoparticles for biomedical applications, Biomaterials 26(18) (2005) 3995-4021.

[2] R. Jin, C. Zeng, M. Zhou, Y. Chen, Atomically Precise Colloidal Metal Nanoclusters and Nanoparticles: Fundamentals and Opportunities, Chem Rev 116(18) (2016) 10346-413.

[3] Q.A. Pankhurst, J. Connolly, S.K. Jones, J. Dobson, Applications of magnetic nanoparticles in biomedicine, J. Phys. D-Appl. Phys. 36(13) (2003) R167-R181.

[4] R.D. Handy, R. Owen, E. Valsami-Jones, The ecotoxicology of nanoparticles and nanomaterials: current status, knowledge gaps, challenges, and future needs, Ecotoxicology 17(5) (2008) 315-325.

[5] S. Panneerselvam, S. Choi, Nanoinformatics: Emerging Databases and Available Tools, International Journal of Molecular Sciences 15(5) (2014) 7158-7182.

[6] G. Cao, Nanostructures & nanomaterials: synthesis, properties & applications, Imperial college press2004.

[7] Y. Wang, Y. Xia, Bottom-up and top-down approaches to the synthesis of monodispersed spherical colloids of low melting-point metals, Nano letters 4(10) (2004) 2047-2050.

[8] V.K. Lamer, R.H. Dinegar, THEORY, PRODUCTION AND MECHANISM OF FORMATION OF MONODISPERSED HYDROSOLS, J. Am. Chem. Soc. 72(11) (1950) 4847-4854.

[9] J. Turkevich, P.C. Stevenson, J. Hillier, A study of the nucleation and growth processes in the synthesis of colloidal gold, Discussions of the Faraday Society 11(11) (1951) 55.

[10] M.C. Daniel, D. Astruc, Gold nanoparticles: Assembly, supramolecular chemistry, quantum-size-related properties, and applications toward biology, catalysis, and nanotechnology, Chemical Reviews 104(1) (2004) 293-346.

[11] P. Reiss, J. Bleuse, A. Pron, Highly luminescent CdSe/ZnSe core/shell nanocrystals of low size dispersion, Nano Letters 2(7) (2002) 781-784.

[12] S.M. Dizaj, A. Mennati, S. Jafari, K. Khezri, K. Adibkia, Antimicrobial Activity of Carbon-Based Nanoparticles, Adv. Pharm. Bull. 5(1) (2015) 19-23.

[13] J.P. Rao, K.E. Geckeler, Polymer nanoparticles: Preparation techniques and size-control parameters, Prog. Polym. Sci. 36(7) (2011) 887-913.

[14] C.J.H. Porter, N.L. Trevaskis, W.N. Charman, Lipids and lipid-based formulations: optimizing the oral delivery of lipophilic drugs, Nat. Rev. Drug Discov. 6(3) (2007) 231-248.

[15] J. Boken, P. Khurana, S. Thatai, D. Kumar, S. Prasad, Plasmonic nanoparticles and their analytical applications: A review, Appl. Spectrosc. Rev. 52(9) (2017) 774-820.

[16] X. Michalet, F.F. Pinaud, L.A. Bentolila, J.M. Tsay, S. Doose, J.J. Li, G. Sundaresan, A.M. Wu, S.S. Gambhir, S. Weiss, Quantum dots for live cells, in vivo imaging, and diagnostics, Science 307(5709) (2005) 538-544.

[17] P. Tartaj, M.D. Morales, S. Veintemillas-Verdaguer, T. Gonzalez-Carreno, C.J. Serna, The preparation of magnetic nanoparticles for applications in biomedicine, J. Phys. D-Appl. Phys. 36(13) (2003) R182-R197.

[18] A.H. Lu, E.L. Salabas, F. Schuth, Magnetic nanoparticles: Synthesis, protection, functionalization, and application, Angewandte Chemie-International Edition 46(8) (2007) 1222-1244.

[19] X.Y. Gao, H. Matsui, Peptide-based nanotubes and their applications in bionanotechnology, Advanced Materials 17(17) (2005) 2037-2050.

[20] H. Matsui, P. Porrata, G.E. Douberly, Protein tubule immobilization on self-assembled monolayers on Au substrates, Nano Letters 1(9) (2001) 461-464.

[21] B. Khodashenas, H.R.J.A.J.o.C. Ghorbani, Synthesis of silver nanoparticles with different shapes, (2015).

[22] Y. Sun, Y. Xia, Shape-controlled synthesis of gold and silver nanoparticles, Science 298(5601) (2002) 2176-9.

[23] Y. Zhou, C. Wang, Y. Zhu, Z.J.C.o.m. Chen, A novel ultraviolet irradiation technique for shape-controlled synthesis of gold nanoparticles at room temperature, 11(9) (1999) 2310-2312.

[24] M. Sastry, Phase transfer protocols in nanoparticle synthesis, CURRENT SCIENCE-BANGALORE- 85(12) (2003) 1735-1745.

[25] J. Hühn, C. Carrillo-Carrion, M.G. Soliman, C. Pfeiffer, D. Valdeperez, A. Masood, I. Chakraborty, L. Zhu, M. Gallego, Z. Yue, Selected standard protocols for the synthesis, phase transfer, and characterization of inorganic colloidal nanoparticles, Chemistry of Materials 29(1) (2016) 399-461.

[26] P. Kunwar, J. Hassinen, G. Bautista, R.H.A. Ras, J. Toivonen, Direct Laser Writing of Photostable Fluorescent Silver Nanoclusters in Polymer Films, ACS Nano 8(11) (2014) 11165-11171.

[27] P. Kunwar, J. Hassinen, G. Bautista, R.H.A. Ras, J. Toivonen, Sub-micron scale patterning of fluorescent silver nanoclusters using low-power laser, Sci Rep 6 (2016) 6.

[28] R.C. Jin, C.J. Zeng, M. Zhou, Y.X. Chen, Atomically Precise Colloidal Metal Nanoclusters and Nanoparticles: Fundamentals and Opportunities, Chemical Reviews 116(18) (2016) 10346-10413.

[29] I.P. Suzdalev, P.I. Suzdalev, Nanoclusters and nanocluster systems. Assembling, interactions, properties, Uspekhi Khimii 70(3) (2001) 203-240.

[30] F. Baletto, R. Ferrando, Structural properties of nanoclusters: Energetic, thermodynamic, and kinetic effects, Rev. Mod. Phys. 77(1) (2005) 371-423.

[31] B.K. Teo, N.J.A. Sloane, MAGIC NUMBERS IN POLYGONAL AND POLYHEDRAL CLUSTERS, Inorganic Chemistry 24(26) (1985) 4545-4558.

[32] I. Díez, M. Pusa, S. Kulmala, H. Jiang, A. Walther, A.S. Goldmann, A.H. Müller, O. Ikkala, R.H. Ras, Color tunability and electrochemiluminescence of silver nanoclusters, Angewandte Chemie International Edition 48(12) (2009) 2122-2125.

[33] Y. Lu, W. Chen, Sub-nanometre sized metal clusters: from synthetic challenges to the unique property discoveries, Chem Soc Rev 41(9) (2012) 3594-623.

[34] G. Storm, S.O. Belliot, T. Daemen, D.D. Lasic, SURFACE MODIFICATION OF NANOPARTICLES TO OPPOSE UPTAKE BY THE MONONUCLEAR PHAGOCYTE SYSTEM, Adv. Drug Deliv. Rev. 17(1) (1995) 31-48.

[35] L. Wang, L.L. Li, Y.S. Fan, H. Wang, Host-Guest Supramolecular Nanosystems for Cancer Diagnostics and Therapeutics, Advanced Materials 25(28) (2013) 3888-3898.

[36] O.V. Salata, Applications of nanoparticles in biology and medicine, Journal of nanobiotechnology 2(1) (2004) 3.

[37] J. Panyam, V. Labhasetwar, Biodegradable nanoparticles for drug and gene delivery to cells and tissue, Adv. Drug Deliv. Rev. 55(3) (2003) 329-347.

[38] E.C. Dreaden, A.M. Alkilany, X.H. Huang, C.J. Murphy, M.A. El-Sayed, The golden age: gold nanoparticles for biomedicine, Chem. Soc. Rev. 41(7) (2012) 2740-2779.

[39] F. Wang, D. Banerjee, Y.S. Liu, X.Y. Chen, X.G. Liu, Upconversion nanoparticles in biological labeling, imaging, and therapy, Analyst 135(8) (2010) 1839-1854.

[40] L. Shang, S. Dong, G.U. Nienhaus, Ultra-small fluorescent metal nanoclusters: synthesis and biological applications, Nano Today 6(4) (2011) 401-418.

[41] L. Zhang, E. Wang, Metal nanoclusters: new fluorescent probes for sensors and bioimaging, Nano Today 9(1) (2014) 132-157.

[42] C. Wang, Y. Wang, L. Xu, D. Zhang, M. Liu, X. Li, H. Sun, Q. Lin, B. Yang, Facile Aqueous‐Phase Synthesis of Biocompatible and Fluorescent Ag2S Nanoclusters for Bioimaging: Tunable Photoluminescence from Red

to Near Infrared, Small 8(20) (2012) 3137-3142.
[43] M.E. Vance, T. Kuiken, E.P. Vejerano, S.P. McGinnis, M.F. Hochella, D. Rejeski, M.S. Hull, Nanotechnology in the real world: Redeveloping the nanomaterial consumer products inventory, Beilstein J. Nanotechnol. 6 (2015) 1769-1780.
[44] M.E. Vance, T. Kuiken, E.P. Vejerano, S.P. McGinnis, M.F. Hochella, Jr., D. Rejeski, M.S. Hull, Nanotechnology in the real world: Redeveloping the nanomaterial consumer products inventory, Beilstein J Nanotechnol 6 (2015) 1769-80.
[45] P. Rivera-Gil, D. Jimenez De Aberasturi, V. Wulf, B. Pelaz, P. Del Pino, Y. Zhao, J.M. De La Fuente, I. Ruiz De Larramendi, T. Rojo, X.-J. Liang, W.J. Parak, The Challenge To Relate the Physicochemical Properties of Colloidal Nanoparticles to Their Cytotoxicity, Accounts Chem. Res. 46(3) (2013) 743-749.
[46] X.J. Wang, S.P. Reece, J.M. Brown, Immunotoxicological impact of engineered nanomaterial exposure: mechanisms of immune cell modulation, Toxicol. Mech. Methods 23(3) (2013) 168-177.
[47] Q. Mu, G. Jiang, L. Chen, H. Zhou, D. Fourches, A. Tropsha, B. Yan, Chemical basis of interactions between engineered nanoparticles and biological systems, Chem Rev 114(15) (2014) 7740-81.
[48] C. Buzea, Pacheco, II, K. Robbie, Nanomaterials and nanoparticles: Sources and toxicity, Biointerphases 2(4) (2007) MR17-MR71.
[49] N. Lewinski, V. Colvin, R. Drezek, Cytotoxicity of nanoparticles, Small 4(1) (2008) 26-49.
[50] W.H. De Jong, P.J. Borm, Drug delivery and nanoparticles: applications and hazards, International journal of nanomedicine 3(2) (2008) 133.
[51] G. Oberdorster, E. Oberdorster, J. Oberdorster, Nanotoxicology: An emerging discipline evolving from studies of ultrafine particles, Environ. Health Perspect. 113(7) (2005) 823-839.
[52] Y. Zhou, G. Quan, Q. Wu, X. Zhang, B. Niu, B. Wu, Y. Huang, X. Pan, C.J.A.p.s.B. Wu, Mesoporous silica nanoparticles for drug and gene delivery, 8(2) (2018) 165-177.
[53] M. Karimi, A. Ghasemi, P.S. Zangabad, R. Rahighi, S.M.M. Basri, H. Mirshekari, M. Amiri, Z.S. Pishabad, A. Aslani, M.J.C.S.R. Bozorgomid, Smart micro/nanoparticles in stimulus-responsive drug/gene delivery systems, 45(5) (2016) 1457-1501.
[54] P.K. Jain, K.S. Lee, I.H. El-Sayed, M.A.J.T.j.o.p.c.B. El-Sayed, Calculated absorption and scattering properties of gold nanoparticles of different size, shape, and composition: applications in biological imaging and biomedicine, 110(14) (2006) 7238-7248.
[55] V. Amendola, M. Meneghetti, Size Evaluation of Gold Nanoparticles by UV-vis Spectroscopy, Journal of Physical Chemistry C 113(11) (2009) 4277-4285.
[56] R. Begum, Z.H. Farooqi, K. Naseem, F. Ali, M. Batool, J.L. Xiao, A. Irfan, Applications of UV/Vis Spectroscopy in Characterization and Catalytic Activity of Noble Metal Nanoparticles Fabricated in Responsive Polymer Microgels: A Review, Crit. Rev. Anal. Chem. 48(6) (2018) 503-516.
[57] A.M. LeQuang, A. Yaacoub, B. Mellis, Characterization of gold nanoparticles in size and concentration by UV-Vis spectroscopy, Abstr. Pap. Am. Chem. Soc. 243 (2012) 1.
[58] W. Haiss, N.T.K. Thanh, J. Aveyard, D.G. Fernig, Determination of size and concentration of gold nanoparticles from UV-Vis spectra, Analytical chemistry 79(11) (2007) 4215-4221.
[59] D. Paramelle, A. Sadovoy, S. Gorelik, P. Free, J. Hobley, D.G. Fernig, A rapid method to estimate the concentration of citrate capped silver nanoparticles from UV-visible light spectra, Analyst 139(19) (2014) 4855-4861.
[60] W. Haiss, N.T. Thanh, J. Aveyard, D.G. Fernig, Determination of size and concentration of gold nanoparticles from UV-vis spectra, Analytical chemistry 79(11) (2007) 4215-21.
[61] K. Naseem, M.A.U. Rehman, R. Huma, Review on vinyl acetic acid-based polymer microgels for

biomedical and other applications, Int. J. Polym. Mater. Polym. Biomat. 67(5) (2018) 322-332.
[62] Q. Wang, Y.B. Zhao, H.B. Xu, X.L. Yang, Y.J. Yang, Thermosensitive Phase Transition Kinetics of Poly(N-isopropylacryl amide-co-acrylamide) Microgel Aqueous Dispersions, J. Appl. Polym. Sci. 113(1) (2009) 321-326.
[63] J.H. Kim, T.R. Lee, Hydrogel-templated growth of large gold nanoparticles: Synthesis of thermally responsive hydrogel-nanoparticle composites, Langmuir 23(12) (2007) 6504-6509.
[64] R. Contreras-Caceres, C. Dawson, P. Formanek, D. Fischer, F. Simon, A. Janke, P. Uhlmann, M. Stamm, Polymers as Templates for Au and Au@Ag Bimetallic Nanorods: UV-Vis and Surface Enhanced Raman Spectroscopy, Chem. Mat. 25(2) (2013) 158-169.
[65] K. Siskova, K. Safarova, J.H. Seo, R. Zboril, M. Mashlan, Non-chemical approach toward 2D self-assemblies of Ag nanoparticles via cold plasma treatment of substrates, Nanotechnology 22(27) (2011) 7.
[66] E.E. Finney, R.G. Finke, Nanocluster nucleation and growth kinetic and mechanistic studies: A review emphasizing transition-metal nanoclusters, J. Colloid Interface Sci. 317(2) (2008) 351-374.
[67] J. Lyklema, Fundamentals of interface and colloid science. Volume 2: Solid-liquid interfaces. With special contributions by A. de Keizer, BH Bijsterbosch, GJ Fleer and MA Cohen Stuart, (1995).
[68] R.J. Hunter, Zeta potential in colloid science: principles and applications, Academic press2013.
[69] J.D. Clogston, A.K. Patri, Zeta potential measurement, Characterization of nanoparticles intended for drug delivery, Springer2011, pp. 63-70.
[70] A. Schwartz, L. Wang, E. Early, A. Gaigalas, Y.-z. Zhang, G.E. Marti, R.F.J.J.o.r.o.t.N.I.o.S. Vogt, Technology, Quantitating fluorescence intensity from fluorophore: The definition of MESF assignment, 107(1) (2002) 83.
[71] L. Zhu, B. Pelaz, I. Chakraborty, W.J.J.I.j.o.m.s. Parak, Investigating Possible Enzymatic Degradation on Polymer Shells around Inorganic Nanoparticles, 20(4) (2019) 935.
[72] N. Feliu, D. Docter, M. Heine, P. del Pino, S. Ashraf, J. Kolosnjaj-Tabi, P. Macchiarini, P. Nielsen, D. Alloyeau, F.J.C.S.R. Gazeau, In vivo degeneration and the fate of inorganic nanoparticles, 45(9) (2016) 2440-2457.
[73] S.J. Soenen, U. Himmelreich, N. Nuytten, T.R. Pisanic, A. Ferrari, M.J.S. De Cuyper, Intracellular nanoparticle coating stability determines nanoparticle diagnostics efficacy and cell functionality, 6(19) (2010) 2136-2145.
[74] P. Rivera-Gil, D. Jimenez De Aberasturi, V. Wulf, B. Pelaz, P. Del Pino, Y. Zhao, J.M. De La Fuente, I. Ruiz De Larramendi, T. Rojo, X.-J.J.A.o.c.r. Liang, The challenge to relate the physicochemical properties of colloidal nanoparticles to their cytotoxicity, 46(3) (2012) 743-749.
[75] L.B.J.B.C. Spector, Covalent enzyme-substrate intermediates in transferase reactions, 2(4) (1973) 311-321.
[76] V. Sée, P. Free, Y. Cesbron, P. Nativo, U. Shaheen, D.J. Rigden, D.G. Spiller, D.G. Fernig, M.R. White, I.A.J.A.n. Prior, Cathepsin L digestion of nanobioconjugates upon endocytosis, 3(9) (2009) 2461-2468.
[77] T. Akagi, M. Higashi, T. Kaneko, T. Kida, M.J.B. Akashi, Hydrolytic and enzymatic degradation of nanoparticles based on amphiphilic poly (γ-glutamic acid)-graft-L-phenylalanine copolymers, 7(1) (2006) 297-303.
[78] R. De La Rica, D. Aili, M.M.J.A.d.d.r. Stevens, Enzyme-responsive nanoparticles for drug release and diagnostics, 64(11) (2012) 967-978.
[79] N. Qiu, X. Liu, Y. Zhong, Z. Zhou, Y. Piao, L. Miao, Q. Zhang, J. Tang, L. Huang, Y.J.A.M. Shen, Esterase‐Activated Charge‐Reversal Polymer for Fibroblast‐Exempt Cancer Gene Therapy, 28(48) (2016) 10613-10622.
[80] C. Zhang, Essential functions of iron-requiring proteins in DNA replication, repair and cell cycle control, Protein Cell 5(10) (2014) 750-60.

[81] T. Yang, C. Shen, Z. Li, H. Zhang, C. Xiao, S. Chen, Z. Xu, D. Shi, J. Li, H.J.T.J.o.P.C.B. Gao, Highly ordered self-assembly with large area of Fe3O4 nanoparticles and the magnetic properties, 109(49) (2005) 23233-23236.

[82] S. Prijic, G. Sersa, Magnetic nanoparticles as targeted delivery systems in oncology, Radiology and Oncology 45(1) (2011) 1-16.

[83] Y.W. Jun, J.H. Lee, J. Cheon, Chemical design of nanoparticle probes for high-performance magnetic resonance imaging, Angew. Chem.-Int. Edit. 47(28) (2008) 5122-5135.

[84] A.K. Gupta, M.J.b. Gupta, Synthesis and surface engineering of iron oxide nanoparticles for biomedical applications, 26(18) (2005) 3995-4021.

[85] M. Mahdavi, M.B. Ahmad, M.J. Haron, F. Namvar, B. Nadi, M.Z.A. Rahman, J.J.M. Amin, Synthesis, surface modification and characterisation of biocompatible magnetic iron oxide nanoparticles for biomedical applications, 18(7) (2013) 7533-7548.

[86] M.R. Saboktakin, R.M. Tabatabaie, A. Maharramov, M.A. Ramazanov, A synthetic macromolecule as MRI detectable drug carriers: Aminodextran-coated iron oxide nanoparticles, Carbohydr. Polym. 80(3) (2010) 695-698.

[87] R. Jin, B. Lin, D. Li, H. Ai, Superparamagnetic iron oxide nanoparticles for MR imaging and therapy: design considerations and clinical applications, Curr Opin Pharmacol 18 (2014) 18-27.

[88] S. Sun, H. Zeng, D.B. Robinson, S. Raoux, P.M. Rice, S.X. Wang, G.J.J.o.t.A.C.S. Li, Monodisperse mfe2o4 (m= fe, co, mn) nanoparticles, 126(1) (2004) 273-279.

[89] H. Chen, P. Zou, J. Connarn, H. Paholak, D.J.N.R. Sun, Intracellular dissociation of a polymer coating from nanoparticles, 5(11) (2012) 815-825.

[90] D.J.B.r. Koshland Jr, Stereochemistry and the mechanism of enzymatic reactions, 28(4) (1953) 416-436.

[91] A.L. Menefee, T.N.J.T.F.j. Zeczycki, Nearly 50 years in the making: defining the catalytic mechanism of the multifunctional enzyme, pyruvate carboxylase, 281(5) (2014) 1333-1354.

[92] K. Hult, P. Berglund, Enzyme promiscuity: mechanism and applications, Trends Biotechnol 25(5) (2007) 231-8.

[93] C.-A.J. Lin, T.-Y. Yang, C.-H. Lee, S.H. Huang, R.A. Sperling, M. Zanella, J.K. Li, J.-L. Shen, H.-H. Wang, H.-I.J.A.n. Yeh, Synthesis, characterization, and bioconjugation of fluorescent gold nanoclusters toward biological labeling applications, 3(2) (2009) 395-401.

[94] I. Diez, R.H.A. Ras, Fluorescent silver nanoclusters, Nanoscale 3(5) (2011) 1963-1970.

[95] D.M. Chevrier, A. Chatt, P.J.J.o.N. Zhang, Properties and applications of protein-stabilized fluorescent gold nanoclusters: short review, 6(1) (2012) 064504.

[96] J. Zheng, C. Zhou, M. Yu, J.J.N. Liu, Different sized luminescent gold nanoparticles, 4(14) (2012) 4073-4083.

[97] Z. Wu, R.J.N.l. Jin, On the ligand's role in the fluorescence of gold nanoclusters, 10(7) (2010) 2568-2573.

[98] G. Pramanik, J. Humpolickova, J. Valenta, P. Kundu, S. Bals, P. Bour, M. Dracinsky, P.J.N. Cigler, Gold nanoclusters with bright near-infrared photoluminescence, 10(8) (2018) 3792-3798.

[99] C.C. Huang, Z. Yang, K.H. Lee, H.T. Chang, Synthesis of highly fluorescent gold nanoparticles for sensing mercury (II), Angewandte Chemie 119(36) (2007) 6948-6952.

[100] X. Yuan, N. Goswami, W. Chen, Q. Yao, J.J.C.C. Xie, Insights into the effect of surface ligands on the optical properties of thiolated Au 25 nanoclusters, 52(30) (2016) 5234-5237.

[101] D. Cao, J. Fan, J. Qiu, Y. Tu, J.J.B. Yan, Bioelectronics, Masking method for improving selectivity of gold nanoclusters in fluorescence determination of mercury and copperions, 42 (2013) 47-50.

[102] S.X. Wang, Q. Li, X. Kang, M.Z. Zhu, Customizing the Structure, Composition, and Properties of Alloy

Nanoclusters by Metal Exchange, Accounts Chem. Res. 51(11) (2018) 2784-2792.
[103] J.-P. Choi, C.A. Fields-Zinna, R.L. Stiles, R. Balasubramanian, A.D. Douglas, M.C. Crowe, R.W.J.T.J.o.P.C.C. Murray, Reactivity of [Au25 (SCH2CH2Ph) 18] 1− nanoparticles with metal ions, 114(38) (2010) 15890-15896.
[104] G. Rossi, R. Ferrando, A. Rapallo, A. Fortunelli, B.C. Curley, L.D. Lloyd, R.L.J.T.J.o.c.p. Johnston, Global optimization of bimetallic cluster structures. II. Size-matched Ag-Pd, Ag-Au, and Pd-Pt systems, 122(19) (2005) 194309.
[105] Y.-C. Shiang, C.-C. Huang, H.-T.J.C.C. Chang, Gold nanodot-based luminescent sensor for the detection of hydrogen peroxide and glucose, (23) (2009) 3437-3439.
[106] B.Y. Han, E.K. Wang, DNA-templated fluorescent silver nanoclusters, Anal. Bioanal. Chem. 402(1) (2012) 129-138.
[107] Y.T. Chen, T.Q. Yang, H.F. Pan, Y.F. Yuan, L. Chen, M.W. Liu, K. Zhang, S.J. Zhang, P. Wu, J.H. Xu, Photoemission Mechanism of Water-Soluble Silver Nanoclusters: Ligand-to-Metal-Metal Charge Transfer vs Strong Coupling between Surface Plasmon and Emitters, J. Am. Chem. Soc. 136(5) (2014) 1686-1689.
[108] M. Walter, J. Akola, O. Lopez-Acevedo, P.D. Jadzinsky, G. Calero, C.J. Ackerson, R.L. Whetten, H. Grönbeck, H.J.P.o.t.N.A.o.S. Häkkinen, A unified view of ligand-protected gold clusters as superatom complexes, 105(27) (2008) 9157-9162.
[109] Q. Li, M. Zhou, W.Y. So, J. Huang, M. Li, D.R. Kauffman, M. Cotlet, T. Higaki, L.A. Peteanu, Z.J.J.o.t.A.C.S. Shao, A Mono-Cuboctahedral Series of Gold Nanoclusters: Photoluminescence Origin, Large Enhancement, Wide Tunability and Structure-Property Correlation, (2019).
[110] G. Soldan, M.A. Aljuhani, M.S. Bootharaju, L.G. AbdulHalim, M.R. Parida, A.H. Emwas, O.F. Mohammed, O.M.J.A.C.I.E. Bakr, Gold Doping of Silver Nanoclusters: A 26‐Fold Enhancement in the Luminescence Quantum Yield, 55(19) (2016) 5749-5753.
[111] B. Adhikari, A.J.C.o.M. Banerjee, Facile synthesis of water-soluble fluorescent silver nanoclusters and HgII sensing, 22(15) (2010) 4364-4371.
[112] C. Wang, L. Xu, X. Xu, H. Cheng, H. Sun, Q. Lin, C.J.J.o.c. Zhang, i. science, Near infrared Ag/Au alloy nanoclusters: tunable photoluminescence and cellular imaging, 416 (2014) 274-279.
[113] C. Zheng, A.-X. Zheng, B. Liu, X.-L. Zhang, Y. He, J. Li, H.-H. Yang, G.J.C.C. Chen, One-pot synthesized DNA-templated Ag/Pt bimetallic nanoclusters as peroxidase mimics for colorimetric detection of thrombin, 50(86) (2014) 13103-13106.
[114] I. Chakraborty, T.J.N. Pradeep, Reversible formation of Ag 44 from selenolates, 6(23) (2014) 14190-14194.
[115] X. Qu, Y. Li, L. Li, Y. Wang, J. Liang, J.J.J.o.N. Liang, Fluorescent gold nanoclusters: synthesis and recent biological application, 2015 (2015) 4.

Eidesstattliche Erklärung

Hiermit erkläre ich an Eides statt, dass ich die vorliegende Dissertationsschrift selbst verfasst und keine anderen als die angegebenen Quellen und Hilfsmittel benutzt habe.

Hamburg, den 25. April 2019 Lin Zhu